

1 **Referee 1**

2

3 Many thanks for the constructive suggestions. Our responses are in red text  
4 below.

5

6 The paper describes PLASIM-GENIE a new intermediate-complexity  
7 Atmosphere- Ocean Earth System Model, designed for simulations of millenium+  
8 length. The new model is well suited for studies of long-term climate change, its  
9 simulation of present-day climate is acceptable, its formulation is mostly  
10 described well, and I recommend publication subject to the following changes  
11 being made.

12

13 1. It's not 100% clear whether or not this model has a carbon cycle, and what  
14 aspects of this are turned on or off. The model is described as an AOGCM  
15 (suggesting no C-cycle), but section 2.1 and others do allude to the simulation of  
16 different carbon pools on land, which is slightly confusing. I presume there is  
17 some sort of diagnostic C-cycle which does not affect atmospheric CO<sub>2</sub>, but does  
18 affect vegetation. However GENIE- 1 does contain a fully interactive C-cycle. The  
19 abstract, introduction, section 2.1 and other sections have to be clearer about  
20 which parts of the C-cycle are on or off. Any flexibility in the C-cycle (ie: being  
21 run in a diagnostic mode to simulation terrestrial pools but without affecting the  
22 ocean and atmosphere) should be noted, as potential users of this AOGCM would  
23 be interested in this.

24

25 As suggested, we have added flexibility to the run the terrestrial carbon cycle in  
26 diagnostic mode. If parameter *nbiome* is set to 2, the calculation of land surface  
27 characteristics depends only upon the initialised vegetation state (e.g. from an  
28 existing spin-up), but the vegetation is allowed to dynamically evolve.

29

30 "ENTS can be run in a diagnostic mode (setting parameter *nbiome*=2), simulating  
31 terrestrial carbon pools without affecting the climate state."

32

33 We have now clarified in the abstract and introduction that the coupling is only  
34 to the physical components of the GENIE framework. Additionally we have  
35 added explanatory text in section 2.1:

36

37 "We note that although ENTS is formulated in terms of carbon densities, we  
38 have not coupled PLASIM-ENTS to the GENIE-1 carbon cycle; this extension is  
39 straightforward in principle and will be addressed in future work."

40

41 2. What is the difference between PLASIM-GENIE and OSU-Vic? Is the UVic ocean  
42 component a frictional geostrophic model like GENIE? OSU-UVic is also  
43 downloadable, so potential users of PLASIM-GENIE should know the differences  
44 between the two.

45

46 We have clarified with the additional text in section 4.1.1:

47

48 "The most significant difference between PLASIM-GENIE and USOVic is the  
49 differing complexity of the ocean models; USO-Vic incorporates the more

50 complex primitive-equation Modular Ocean Model (MOM) version 2.2  
51 (Pacanowski 1995) at a horizontal resolution of  $1.8^\circ \times 3.6^\circ$ . The primitive  
52 equations include momentum advection terms neglected in our system.”

53

54 3. The following parameterisations in section 2.1 need to be clarified/described  
55 in more detail (a sentence or two on each will do): -"shortwave and longwave  
56 radiative transport"; this is a very confusing term and in particular needs  
57 clarifying -"interactive clouds"; are these based on relative humidity? -"diffusive  
58 transport"; I guess this is some sort of hyperdiffusion? -how many visible and IR  
59 bands are there in PLASIM's radiation scheme?

60

61 We have now expanded the description of parameterisations in section 2.1:

62

63 “PLASIM (Fraedrich 2012) is a reduced complexity AGCM, with the 3D primitive  
64 equation atmosphere model PUMA at its core (Fraedrich et al 2005). PLASIM is  
65 described in detail in Lunkeit et al (2007) and references therein. We summarise  
66 briefly here. The atmospheric dynamics are solved using the spectral transform  
67 method, formulated for temperature, log surface pressure, divergence and  
68 vorticity. The short wave radiation scheme separates solar radiation into two  
69 bands,  $\lambda < 0.75 \mu\text{m}$  (with cloud scattering, ozone absorption and Rayleigh  
70 scattering) and  $\lambda > 0.75 \mu\text{m}$  (with cloud scattering, cloud absorption and water  
71 vapour absorption). The long wave radiation scheme uses the broad band  
72 emissivity method, with the (greenhouse gas) effect of water vapour, carbon  
73 dioxide and ozone included in the calculation of emissivity. Ozone concentration  
74 is prescribed with an analytic spatio-temporal distribution. Cloud emissivity is  
75 calculated from the cloud liquid water content. Fractional cloud cover is  
76 diagnosed from relative humidity (stratiform clouds) and from the convective  
77 precipitation rate (convective clouds). Other parameterised processes include  
78 large-scale precipitation, moist convection (both cumulus and shallow), dry  
79 convection, boundary layer heat fluxes, vertical diffusion (to represent  
80 unresolved turbulent exchange) and horizontal diffusion (applied to selectively  
81 dampen short wavelengths in spectral space).”

82

83 4. Section 3.2: Radiation and convection seem to account for a very large  
84 percent- age of the CPU load: potential users might want to replace the radiative  
85 scheme with something that is quicker- but also more general and flexible, e.g. a  
86 simpler semi-grey scheme (e.g. one LW band emits from the surface, one from  
87 the atmosphere depend- ing on some simplified optical depth). Could the authors  
88 add a sentence on how easy this might be to do (from the point of view  
89 increasing this model's potential user base)

90

91 We have added text in section 3:

92

93 “We note that the modular structure of PLASIM means that replacing the  
94 radiation scheme with, for example, a computationally fast semi-grey scheme  
95 (Frierson et al 2006) would be relatively straightforward. An efficient convective  
96 adjustment scheme (Betts and Miller 1986) is already available as an alternative  
97 to the default moisture budget scheme (Kuo 1965, 1974).”

98

99 5. Section 3.3: Why does conversion from PE to KE necessarily cause an energy  
100 imbalance? This should be explained in detail- or at the very least a citation to  
101 other work that clearly explains why the imbalance happens should be included.  
102

103 We have added explanatory text in section 3.3:

104  
105 “We note that the PLASIM atmosphere does not precisely conserve energy, as  
106 illustrated by Hoskins and Simmons (1975) for a similar dry dynamical core. The  
107 largest effect in PLASIM comes from the conversion from potential to kinetic  
108 energy. This conversion cannot be formulated in a conservative manner in the  
109 semi-spectral scheme since it involves triple products while the (Gaussian) grid  
110 only allows for the conservation of quadratic quantities.”  
111

112 6. Figures 2,3,4: it is very hard to see what the differences between model and  
113 reanalysis are without difference plots. Contours plots of differences between  
114 PLASIM-GENIE and reanalysis need to be made for these three figures so readers  
115 can see what and where they are for themselves.  
116

117 Difference plots have been added to Figures 2, 3, and 4.

118  
119 7. Suggestion: the simulation of aridity seems pretty good- the authors might  
120 want to state the simulation of aridity in the abstract so potential users who are  
121 interested in model/observations comparisons are more likely to investigate the  
122 rest of the paper.  
123

124 Text added to abstract:

125  
126 “The simulated climate is presented considering (i) global fields of seasonal  
127 surface air temperature, precipitation, wind, solar and thermal radiation, with  
128 comparisons to reanalysis data; (ii) vegetation carbon, soil moisture and aridity  
129 index; (iii) sea surface temperature, salinity and the meridional Atlantic and  
130 Pacific streamfunctions. Considering its resolution PLASIM-GENIE reproduces  
131 the main features of the climate system well and demonstrates usefulness for a  
132 wide range of applications.”  
133  
134

135 **Referee 2**

136

137 Many thanks for these constructive suggestions. Our responses are in red below.

138

139 General comments

140

141 The manuscript describes a new coupled atmosphere-ocean model in a rather  
142 compact manner focusing on the parameter tuning. The model should be very  
143 useful for the community and would promise contribution to the scientific  
144 advancement in this field. This aspect is enhanced particularly by the release of  
145 the model. The description of such model with potentially broad application is  
146 useful and deserves to be published in the GMD. The current description is,  
147 however, unsatisfactory in its current form for the reasons listed below.

148

149 Major comments

150

151 1. Quantitative (and physical, in some cases) meaning of some variables  
152 discussed in the manuscript is unclear for the non-GENIE users unless the reader  
153 consults with the multiple previous papers. I do not expect that all variables are  
154 explained in details, but the highlighted variables such as “acllwr”, “albseamax”,  
155 “qthresh” “ADRAG”, and “SCF” need to be expressed with equations. Otherwise,  
156 the discussion on the presented values does not mean much for many potential  
157 readers. The term “sea ice diffusivity” is also unclear although I would imagine  
158 this represents the diffusive effect of unresolved ocean currents (and other  
159 dynamical effect) on the sea ice concentration.

160

161 We have greatly expanded the descriptions of parameters. Section 4.1

162

163 “Parameters from modules other than GOLDSTEIN were all fixed. However, some  
164 were changed from their default values on the basis of exploratory simulations:

165 i)

166 The uncertain effect of clouds on long wave radiation is controlled  
167 through the dependence of cloud emissivity  $A$  on the mass absorption  
factor  $k$  “acllwr”, following Slingo and Slingo (1991):

$$A = 1 - e^{-\beta kW}$$

168

169 where  $\beta = 1.66$  is the diffusivity factor and  $W$  the cloud liquid water  
170 path. The mass absorption factor was found to exert the strongest  
171 control on surface air temperature of the 22 key model parameters  
172 considered in PLASIM-ENTS ensembles (Holden et al 2014). The value  
173 was increased from default  $k = 0.1$  to  $0.2m^2g^{-1}$ , estimated to yield a  
174 simulated global average surface air temperature of approximately  
14°C in conjunction with parameter choices (ii) to (v) below.

175 ii)

176 The PLASIM parameter *albseamax* defines the latitudinal variation of  
ocean albedo (Holden et al 2014),

$$\alpha_s = \alpha_{s0} + 0.5\alpha_{s1}[1 - \cos(2\varphi)]$$

177

178 where the ocean albedo  $\alpha_s$  is expressed in terms of latitude  $\varphi$ , the albedo  
179 at the equator  $\alpha_{s0} = 0.069$  and the parameter that controls latitudinal  
180 variability  $\alpha_{s1}$ . The calculated albedo is applied to both direct and  
181 scattered radiation. A high value ( $\alpha_{s1} = 0.4$ ) was favoured for  
*albseamax*, leading to cooler high latitude ocean and favouring

182 increased Southern Ocean sea-ice and deep-water formation, which  
 183 both tended to be too low with default parameters.

184 iii) Sea ice is transported through advection and Laplacian diffusion  
 185 (Edwards and Marsh, 2005), the latter taking the place of a detailed  
 186 representation of unresolved advection and rheological processes.  
 187 Sea-ice diffusivity (*SID*) influences AABW formation by controlling the  
 188 rate at which new ice is created, and hence the strength of brine  
 189 rejection (Holden et al 2013b). A high value was favoured, again to  
 190 strengthen deep-water formation, but values greater than 15,000 m<sup>2</sup>s<sup>-1</sup>  
 191 were found to lead to numerical instabilities in this model and *SID* was  
 192 fixed at this value.

193 iv) The standard PLASIM expression for the dependence of sea ice albedo  
 194  $\alpha_i$  on surface air temperature is used

$$\alpha_i = 0.5 - 0.025T_{air}$$

195 where  $T_{air}$  is the surface air temperature (°C). PLASIM restricts the  
 196 maximum albedo to 0.7 ( $T_{air} \leq -8^\circ\text{C}$ ). In PLASIM-GENIE we also  
 197 restrict the minimum albedo, 0.5 ( $T_{air} \geq 0^\circ\text{C}$ ).

198 v) The PLASIM-ENTS dependency of photosynthesis on soil moisture is

$$f_2(W_s) = \{(W_s/W_s^*) - q_{th}\} / \{0.75 - q_{th}\}$$

199 The parameter  $q_{th}$  (*qthresh*) was set to 0.1, allowing the development  
 200 of vegetation in semi-arid regions (Holden et al 2014).

201  
 202 The ensemble was generated using a 50x6 maximin latin hypercube design,  
 203 varying six GOLDSTEIN parameters, listed in in Table 1 and varied over ranges  
 204 considered to reflect the plausible range for each parameter (Holden et al 2013b  
 205 and references therein). The six varied parameters are isopycnal and diapycnal  
 206 diffusivities, a parameter *OP1* that controls the depth profile of diapycnal  
 207 diffusivity (see below), the frictional drag coefficient (GOLDSTEIN is based upon  
 208 the thermocline equations with the addition of a linear drag term in the  
 209 horizontal momentum equations, Edwards et al 1998), wind stress scaling (a  
 210 linear scaling of the surface wind-stress is applied to compensate for the energy  
 211 dissipated by frictional drag), and an Atlantic-Pacific moisture flux adjustment.

212  
 213 Diapycnal diffusivity is stratification-dependent (Oliver and Edwards, 2008),  
 214 given by

$$k_v = k_{v0} p_0(z)^\gamma \left( \frac{\Delta\rho_0(z)}{\Delta\rho(z)} \right)$$

215 where  $k_{v0}$  (reference diapycnal diffusivity) and  $\gamma$  (*OP1*) are varied across the  
 216 ensemble (Table 1),  $p_0(z)$  is a reference profile (exponentially growing with  
 217 depth and equal to 1 at 2500m),  $\Delta\rho_0(z)$  a reference vertical density gradient  
 218 profile and  $\Delta\rho(z)$  the local simulated vertical density gradient.”

219  
 220 2. If the APM is a flux-correction parameter, should this depend on the flow? If  
 221 the model simulates the moisture flux correctly, the addition of this flux  
 222 correction would lead to a wrong total moisture flux. This is no longer a  
 223 correction. By design, the flow responds to this parameter “forcing”. I am not  
 224 sure about the physical meaning of this parameter which appears to be an  
 225 important tuning exercise here.

226

227 Apologies, the parameter should have been described as a flux adjustment. This  
228 change has been made throughout. Because the simulated flux is generally  
229 different from the observationally derived values and because of uncertainty in  
230 both the true value of the flux and also its effect on the system, the parameter  
231 plays an important role as a control parameter for the model. It is not clear how  
232 it should be related dynamically to the flow.

233  
234 3. I wonder why the performance of only thermohaline circulation is discussed.  
235 In the introduction, it is mentioned that “dynamic ocean feedbacks are restricted  
236 to the thermohaline circulation” in the previous EMBM coupled version of the  
237 model. Then, the simulated wind-driven circulation and its interaction with the  
238 thermohaline circulation must be one of the selling points of the new model.  
239 Why not discussing the wind driven circulation (and its bias)? Similarly, the sea  
240 ice plays an important role for the thermohaline circulation. Why not discussing  
241 the sea ice distribution (and its bias)?

242  
243 We now consider the influence of wind-driven circulation on the thermohaline  
244 circulation with reference to high-frequency variability, and including additional  
245 Figure 6e:

246  
247 “Figure 6e illustrates wind-driven AMOC variability, behaviour that is absent  
248 from GENIE-1 (Sarojini et al 2011), because it is forced with annual averaged  
249 climatological winds. The maximum Atlantic overturning circulation is plotted  
250 through an arbitrary year (year 100 of a “spin-on” simulation), together with the  
251 100-year mean and standard deviation. “

252  
253 The sea-ice bias is discussed in some detail. A plot is not included as the bias is  
254 very large so that a plot would add little explanatory value:

255  
256 “Sea-ice distributions (not illustrated) exhibit a systematic bias towards low  
257 southern sea-ice area across the ensemble, with an annual average of 2.8 million  
258 km<sup>2</sup> in the subjective tuning; this compares to observational estimates of 11.5  
259 million km<sup>2</sup> (Cavalieri et al 2003). Surface air temperature over the southern  
260 ocean is warm biased with respect to the reanalysis data, despite a modest cold  
261 bias in the global temperature (Figure 2). While this may in part be a  
262 consequence of reduced sea-ice (through the albedo feedback), the continued  
263 presence of the warm bias in southern summer suggests the possibility that the  
264 bias arises in the atmosphere. The decision to control the global temperature  
265 with *acllwr* (Section 4.1) preferentially warms cloudy regions and may have  
266 contributed. Indeed, simulated downward thermal radiation exhibits a  
267 significant bias over the Southern Ocean (Figure 4). A thorough investigation of  
268 the source of this bias is beyond the scope of this study, requiring consideration  
269 of uncertainties in atmospheric and ocean energy transport, and in solar and  
270 thermal radiative transfer, considering clouds, water vapour, and surface  
271 processes.”

272  
273 4. Throughout the manuscript, it is stated that the new model is substantially  
274 improved from the GENIE-1 (e.g., p.10693, l.15). I think it is very useful to show  
275 with figures which part of the simulated climatology is improved.

276

277 Many of the improvements are not manifested in the spun-up climatology, but  
278 rather reflect the inclusion of dynamics that were previously absent (and forced  
279 where necessary), so the improvements are most notably in feedbacks and  
280 dynamical variability. One area of significant improvement in climatology is  
281 moisture transport and precipitation. Additional text:

282

283 “The plotted outputs were chosen to highlight feedbacks that are neglected by  
284 the EMBM, viz. 3D dynamical atmospheric transport, providing greatly  
285 improved precipitation fields and dynamic surface winds (an imposed forcing in  
286 GENIE-1), and interactive clouds (also an imposed forcing field in GENIE-1,  
287 comprising a spatiotemporal cloud albedo field and uniform OLR adjustment.)”

288

289 and

290

291 “The outputs plotted in Figures 3 and 4 were chosen to focus on dynamics that  
292 are entirely absent from GENIE-1: interactive winds and interactive clouds.  
293 While the inclusion of these dynamics is not expected to improve the simulated  
294 climatology (i.e. when compared to simulations that are forced with  
295 climatological fields), their inclusion represents a substantial upgrade through  
296 the capture of important Earth system feedbacks neglected in GENIE-1. “

297

298 and a plot of GENIE-1 vegetative carbon is added for comparison (i.e. 5b,  
299 replacing an ENTS soil carbon plot), together with text

300

301 “An important example of substantial improvement over the climatology of  
302 GENIE-1 is atmospheric moisture transport, previously touched upon in the  
303 context of Figure 2. Figure 5 compares PLASIM-GENIE vegetative carbon (5a)  
304 and GENIE-1 vegetation carbon (5b, data reproduced from Holden et al, 2013a,  
305 Fig 1a) and highlights various aspects of the improved moisture transport. In  
306 GENIE-1, deserts are poorly resolved (too moist) and boreal forest does not  
307 penetrate far into the continental interior of Eurasia (too dry); these are both  
308 shortcomings that arise from diffusive moisture transport (Lenton et al 2006).  
309 Although the deserts of the Southern hemisphere are not well resolved in either  
310 model, the larger deserts of the Northern hemisphere are distinct in PLASIM-  
311 GENIE, while simulated boreal forest penetrates the Eurasian interior.”

312

313 5. In Figs. 2-4, the model bias, i.e., the difference from the NCEP/NCAR reanalysis  
314 should be presented. The model error bar is unknown, otherwise.

315

316 Difference plots have been added to Figs 2-4.

317

318 Minor comments

319 1. p.10680, l.22: “that that” should be “that”?

320 corrected

321

322 2. p.10681, l.15: “transport” should be “transfer”? 3. p.10681, l.26: Please explain  
323 “self-shading”.

324 Corrected and self-shading explained:

325 “ENTS includes a parameterisation of self-shading, so that new photosynthetic  
326 production is channelled into leaf litter when fractional vegetation coverage  
327 approaches 1 and the canopy closes”

328

329 4. p.10687, l.15: Would it be more helpful to plot the equation using the revised  
330 values of 0.5 and 0.7?

331 We have addressed this by simplifying the presentation of the equation and  
332 introducing some additional text (see response to 1).

333

334 5. p.10692, l.15-16: The years of the NCEP/NCAR reanalysis data need to be  
335 stated.

336 6. p.10692, l.16: Which variables are selected? Are these in Table 1? Then,  
337 writing “selected variables (Table 1)” is more helpful.

338 Revised text (comments 5&6):

339 “Figures 2 to 4 compare a selection of PLASIM-GENIE outputs against  
340 NCEP/NCAR reanalysis fields (Kalnay et al 1996). In each case we compare fifty-  
341 year PLASIM-GENIE averages of southern summer (JJA) and northern summer  
342 (DJF) with the corresponding long-term means (1981-2010) of the reanalysis  
343 data. The plotted outputs were chosen to highlight feedbacks neglected by the  
344 EMBM, viz. 3D dynamical transport, giving greatly improved precipitation fields  
345 and providing dynamic surface winds (an imposed forcing in GENIE-1), and  
346 interactive clouds (also an imposed forcing field in GENIE-1, incorporating a  
347 spatiotemporal cloud albedo field and uniform OLR adjustment.)”

348

349 7. Even if the tuned parameters are mostly ocean model parameters, the  
350 description of atmospheric field/circulation and its bias is useful as a description  
351 paper of the new coupled model.

352 A note on atmospheric circulation is added:

353

354 “Our focus here is on the wind-stress coupling and the tuned ocean state. The 3D  
355 atmospheric circulation is also reasonable. To illustrate, the simulated  
356 Southern/Northern hemisphere winter zonal wind jets ( $\sim 44/43 \text{ ms}^{-1}$ ,  
357  $35^{\circ}\text{S}/35^{\circ}\text{N}$ , 150mbar) compare to reanalysis data ( $\sim 41/44 \text{ ms}^{-1}$ ,  $30^{\circ}\text{S}/30^{\circ}\text{N}$ ,  
358 200mbar).”

359

360

361

362

363

364

365

366

367

368

369

370



## 371 **PLASIM-GENIE: a new intermediate complexity AOGCM**

372 P.B. Holden<sup>1</sup>, N.R. Edwards<sup>1</sup>, K. Fraedrich<sup>2</sup>, E. Kirk<sup>3</sup>, F. Lunkeit<sup>3</sup> and X. Zhu<sup>4</sup>

373 <sup>1</sup>Environment, Earth and Ecosystems, The Open University, Walton Hall, Milton  
374 Keynes, MK7 6AA, UK

375 <sup>2</sup>Max Planck Institute of Meteorology, KlimaCampus, Bundesstraße 53, 20146  
376 Hamburg, Germany

377 <sup>3</sup>Meteorological Institute, University of Hamburg, Bundesstraße 55, 20146  
378 Hamburg, Germany

379 <sup>4</sup>Center for Earth System Research and Sustainability (CEN), University of  
380 Hamburg, Grindelberg 5, 20144 Hamburg, Germany

381

### 382 **Abstract**

383 We describe the development, tuning and climate of PLASIM-GENIE, a new  
384 intermediate complexity Atmosphere-Ocean Global Climate Model (AOGCM),  
385 built by coupling the Planet Simulator to the ocean, sea-ice and land-surface  
386 components of the GENIE Earth system model. PLASIM-GENIE supersedes  
387 “GENIE-2”, a coupling of GENIE to the Reading IGCM. The primitive-equation  
388 atmosphere includes chaotic, 3D motion and interactive radiation and clouds,  
389 and dominates the computational load compared to the relatively simpler  
390 frictional-geostrophic ocean, which neglects momentum advection. The model is  
391 most appropriate for long-timescale or large ensemble studies where numerical  
392 efficiency is prioritised, but lack of data necessitates an internally consistent,  
393 coupled calculation of both oceanic and atmospheric fields. A 1,000-year  
394 simulation with PLASIM-GENIE requires approximately two weeks on a single node  
395 of a 2.1GHz AMD 6172 CPU. We demonstrate the tractability of PLASIM-GENIE  
396 ensembles by deriving a “subjective” tuning of the model with a 50-member  
397 ensemble of 1,000-year simulations. The simulated climate is presented considering  
398 (i) global fields of seasonal surface air temperature, precipitation, wind, solar and  
399 thermal radiation, with comparisons to reanalysis data; (ii) vegetation carbon, soil  
400 moisture and aridity index; (iii) sea surface temperature, salinity and the meridional  
401 Atlantic and Pacific streamfunctions. Considering its resolution PLASIM-GENIE  
402 reproduces the main features of the climate system well and demonstrates usefulness  
403 for a wide range of applications.

Phil Holden 8/4/16 15:07

Deleted: -

Phil Holden 8/4/16 15:07

Deleted: earth

Phil Holden 8/4/16 15:07

Deleted: It has been developed to join the limited number of models that bridge

Phil Holden 8/4/16 15:07

Deleted: gap between EMICS with simplified

Phil Holden 8/4/16 15:07

Deleted: dynamics and state of the art AOGCMs

Phil Holden 8/4/16 15:07

Deleted: An important motivation for intermediate complexity models is the evaluation of uncertainty. We here

Phil Holden 8/4/16 15:07

Formatted: English (US)

## 415 | 1. Introduction

416 The Grid-ENabled Integrated Earth system model (GENIE, Lenton et al 2007) has  
417 been developed as a modular framework that allows a spectrum of intermediate  
418 complexity Earth system models to be created by selecting different options for  
419 the various climate and carbon cycle components. Earth system models created  
420 within GENIE have been configured for published studies spanning a wide range  
421 of geological epochs across Paleozoic, Mesozoic and Cenozoic eras. GENIE  
422 framework models are normally capable of integration over multi-millennial  
423 timescales and several of the published studies have involved millions of years of  
424 simulation time combining long runs and large ensembles. The framework has  
425 been designed to be modular to facilitate the coupling of more complex  
426 component modules as available computing power increases.

427

428 Almost invariably, applications of GENIE have used configurations that represent  
429 the atmosphere with a computationally fast energy-moisture-balance-model  
430 (EMBM, Fanning and Weaver 1996). These configurations are generically named  
431 "GENIE-1". Although adequate for many purposes, especially in the context of  
432 global biogeochemical modelling, an EMBM introduces significant structural  
433 weaknesses to (or even rules out) a range of applications. Diffusive single-layer  
434 moisture transport leads to poor precipitation fields that cannot, for instance,  
435 represent convective precipitation or monsoon dynamics. The EMBM applies  
436 prescribed surface wind fields (Edwards and Marsh 2005), defined either from  
437 climatology or from outputs of more complex models, so that dynamic ocean  
438 feedbacks are restricted to the thermohaline circulation. Clouds are represented  
439 through a prescribed albedo field (Lenton et al 2006) and a spatially uniform  
440 adjustment to outgoing longwave radiation OLR (Holden et al 2010), while  
441 uncertain cloud feedbacks on the radiative balance in a changing climate are  
442 represented through a globally uniform temperature dependent adjustment to  
443 OLR (Matthews and Caldeira 2007, Holden et al 2010).

444

445 In an effort to address these shortcomings, the Reading Intermediate General  
446 Circulation Model (IGCM3.1, de Forster et al 2000), a 3D dynamical model of the  
447 atmosphere, was coupled into GENIE (Annan et al 2005, Lenton et al 2007).

449 Unfortunately this realization of the model “GENIE-2” proved problematic and  
450 has only been applied once since these early studies (Holden and Edwards  
451 2010). The coupling with the slab-ocean model was found to exhibit poor  
452 precipitation fields, apparently due to structural deficiencies in the convection  
453 routine (Annan et al 2005). The coupling with the 3D frictional geostrophic  
454 ocean model GOLDSTEIN displays a patchwork-instability and exhibits a low bias  
455 in precipitation over ocean. GENIE-2 requires a large moisture flux correction  
456 (0.79Sv, reversing the sign of the simulated flux) to reconcile freshwater  
457 transport from the Atlantic to the Pacific with reanalysis data (Lenton et al 2007)  
458 and generate an Atlantic overturning circulation. A further shortcoming is that,  
459 on account of technical complications discussed in Section 3.3, the IGCM was not  
460 coupled to the dynamic sea-ice module GOLDSTEINSEAICE, but only to the slab  
461 sea-ice module.

462

463 GENIE-1 has been applied to a wide range of studies, including participation in  
464 the EMIC inter-comparisons that were performed for the two most recent IPCC  
465 reports (Plattner et al 2008, Zickfeld et al 2013). Although GENIE studies have  
466 generally addressed ocean physics, ocean biogeochemistry and the global carbon  
467 cycle, a more recent focus has been the development of emulators for climate  
468 impact assessment (e.g. Labriet et al 2013, Mercure et al 2014). This application  
469 is poorly suited to highly simplified atmospheric models such as the EMBM.  
470 Although the emulation techniques were developed from GENIE-2 simulations  
471 (Holden and Edwards 2010), this first-generation emulator was not considered  
472 sufficiently robust for applications given the poor climatology of the underlying  
473 simulator. Instead, a second-generation emulator (Holden et al 2014) was  
474 developed using the Planet Simulator PLASIM (Fraedrich 2012).

475

476 PLASIM is a reduced complexity AGCM, with the 3D primitive equation atmosphere  
477 model PUMA at its core (Fraedrich et al 2005). We use the PLASIM-ENTS  
478 implementation (Holden et al 2014), which incorporates the same land surface  
479 model as GENIE. Complementary to GENIE-1, PLASIM has been applied in a  
480 range of atmospheric studies, for instance investigating the global entropy  
481 budget (Fraedrich and Lunkeit, 2008), double ITCZ dynamics in an aquaplanet

Phil Holden 8/4/16 15:07

Deleted: it

483 (Dahms et al, 2011), the Permian climate (Roscher et al, 2011) and a snowball  
484 Earth (Micheels and Montenari, 2008). However, although PLASIM simulates  
485 vastly better climatology than the EMBM of GENIE-1, it lacks dynamic  
486 representations of ocean and sea ice (and does not model the carbon cycle) so it  
487 too neglects important Earth system feedbacks.

488

489 We here describe the implementation of a coupling of PLASIM-~~ENTS to the~~  
490 physical components of the GENIE framework. The coupled model "PLASIM-  
491 GENIE" has been developed to join the limited number of models that bridge the  
492 gap between EMICS with simplified atmospheric dynamics and state of the art  
493 AOGCMs. We are aware of three AOGCMs of comparable complexity with  
494 primitive equation atmospheric dynamics: FAMOUS, the reduced resolution  
495 implementation of HadCM3, which simulates 1,000 years in approximately ten  
496 days on eight CPUs (Williams et al, 2013), SPEEDO, comprising a T30 spectral  
497 atmosphere with simplified parameterizations (Molteni 2003) coupled to a  
498 primitive equation ocean model, which simulates 1,000 years in approximately  
499 two weeks on a 3GHz dual core Intel E6850 CPU (Severijns and Hazeleger, 2010)  
500 and OSUVic, a coupling of PLASIM to the UVic Earth system model (Schmittner et  
501 al, 2010). A 1,000-year simulation with PLASIM-GENIE requires approximately  
502 two weeks on a single node of a 2.1GHz AMD 6172 CPU.

503

504 State of the art climate models operate at the limit of available computing power,  
505 so that very few simulations can be performed with these models. An important  
506 motivation for intermediate complexity models is for the evaluation of  
507 uncertainty. We here demonstrate the tractability of PLASIM-GENIE ensembles by  
508 tuning the model with a 50-member ensemble of 1,000-year simulations.

509

## 510 2. Component Modules

511

### 512 2.1 PLASIM-ENTS

513 PLASIM (Fraedrich 2012) is a reduced complexity AGCM, with the 3D primitive  
514 equation atmosphere model PUMA at its core (Fraedrich et al 2005). PLASIM is  
515 described in detail in Lunkeit et al (2007) and references therein. We summarise

Phil Holden 8/4/16 15:07

Deleted: to

Phil Holden 8/4/16 15:07

Deleted: that

Phil Holden 8/4/16 15:07

Formatted: Font color: Auto

518 | briefly here. The atmospheric dynamics are solved using the spectral transform  
519 | method, formulated for temperature, log surface pressure, divergence and vorticity.  
520 | The short wave radiation scheme separates solar radiation into two bands,  $\lambda <$   
521 |  $0.75\mu\text{m}$  (with cloud scattering, ozone absorption and Rayleigh scattering) and  
522 |  $\lambda > 0.75\mu\text{m}$  (with cloud scattering, cloud absorption and water vapour absorption).  
523 | The long wave radiation scheme uses the broad band emissivity method, with the  
524 | (greenhouse gas) effect of water vapour, carbon dioxide and ozone, included in the  
525 | calculation of emissivity. Ozone concentration is prescribed with an analytic spatio-  
526 | temporal distribution. Cloud emissivity is calculated from the cloud liquid water  
527 | content. Fractional cloud cover is diagnosed from relative humidity (stratiform  
528 | clouds) and from the convective precipitation rate (convective clouds). Other  
529 | parameterised processes include large-scale precipitation, moist convection (both  
530 | cumulus and shallow), dry convection, boundary layer heat fluxes, vertical diffusion  
531 | (to represent unresolved turbulent exchange) and horizontal diffusion (applied to  
532 | selectively dampen short wavelengths in spectral space).

533

534 | The land surface scheme was modified (Holden et al 2014) to use GENIE's 'efficient  
535 | numerical terrestrial scheme' ENTS (Williamson et al 2006), partly in anticipation of  
536 | this coupling to GENIE. ENTS models vegetative and soil carbon densities, assuming  
537 | a single plant functional type that has a doubled-peaked temperature response  
538 | (representing boreal and tropical forest). In addition to temperature, the rate of  
539 | photosynthesis depends upon the atmospheric CO<sub>2</sub> concentration and on soil moisture  
540 | availability. ENTS includes a parameterisation of self-shading, so that new  
541 | photosynthetic production is channelled into leaf litter when fractional vegetation  
542 | coverage approaches one and the canopy closes. Land surface albedo, moisture bucket  
543 | capacity and surface roughness are parameterised in terms of the simulated carbon  
544 | pool densities. We note that although ENTS is formulated in terms of carbon  
545 | densities, we have not coupled PLASIM-GENIE to the GENIE-1 carbon cycle; this  
546 | extension is straightforward in principle and will be addressed in future work. In this  
547 | coupling, ENTS can be run in a diagnostic mode (setting parameter *nbiome*=2),  
548 | simulating dynamically changing terrestrial carbon pools without affecting the climate  
549 | state.

550

Phil Holden 8/4/16 15:07

**Deleted:** Parameterized processes include shortwave and longwave radiative transport, interactive clouds, large-scale precipitation, moist

Phil Holden 8/4/16 15:07

**Deleted:** dry convection, boundary layer sensible heat

Phil Holden 8/4/16 15:07

**Deleted:** latent heat fluxes,

Phil Holden 8/4/16 15:07

**Deleted:** diffusive transport. The model accounts for the

Phil Holden 8/4/16 15:07

**Deleted:** effects

Phil Holden 8/4/16 15:07

**Deleted:** , water vapour

Phil Holden 8/4/16 15:07

**Deleted:** .

Phil Holden 8/4/16 15:07

**Deleted:** , and

564 PLASIM includes flux-corrected slab ocean and slab sea-ice models. The coupling  
565 described here (Section 3) replaces these simple models with the 3D dynamical ocean  
566 model GOLDSTEIN and the thermodynamic-dynamical sea ice model  
567 GOLDSTEINSEAICE.

568

## 569 **2.2 GOLDSTEIN**

570 GOLDSTEIN is a 3D frictional-geostrophic ocean model (Edwards and Marsh,  
571 2005; Marsh et al, 2011). GOLDSTEIN is dynamically similar to classical GCMs,  
572 except that it neglects momentum advection and acceleration. Barotropic flow  
573 around Antarctica is derived from linear constraints that arise from integrating  
574 the depth-averaged momentum equations; we here neglect flow through other  
575 straits. Several modifications to the default GOLDSTEIN can be enabled; here we  
576 apply the modified equation of state that includes a parameterisation of  
577 thermobaricity (K. Oliver, personal communication, 2008) and the enhanced  
578 diapycnal mixing scheme (Oliver and Edwards, 2008).

579

## 580 **2.3 GOLDSTEIN SEA ICE**

581 GOLDSTEINSEAICE (Edwards and Marsh, 2005) solves for the fraction of the  
582 ocean surface covered by ice within a grid cell and for the average sea-ice height.  
583 A diagnostic equation is solved for the ice surface temperature. Growth or decay  
584 of sea ice depends on the net heat flux into the ice (Semtner, 1976; Hibler 1979);  
585 sea-ice dynamics consists of advection by surface currents and diffusion. The  
586 thermodynamics of GOLDSTEINSEAICE are summarized in detail in Section 3.3.

587

## 588 **3. Coupling methodology**

589 A schematic of the PLASIM-ENTS/GOLDSTEIN/GOLDSTEINSEAICE 'pl\_go\_gs'  
590 coupling is illustrated in Figure 1.

591

592 In order to avoid the need for interpolation, the coupling was set up to require  
593 the three models have matched horizontal grids. PLASIM has previously been  
594 configured for T21, T31 and T42 resolutions. Here we restrict the coupling to  
595 T21 and use the matched 64x32 GOLDSTEIN grid (Lenton et al 2007). PLASIM  
596 vertical resolution is 10 levels. GOLDSTEIN depth resolution is 32 levels, with

597 bathymetry defined at the resolution of the 8 level configuration. Extension to  
598 other resolutions (horizontal or vertical) is straightforward in principle.

599

600 The computational demands of the coupled model, simulating 75 years per day on a  
601 single node of a 256Gb 2.1GHz AMD 6172 CPU, are dominated by PLASIM (98%).

602 The computational demands of PLASIM are dominated by diabatic processes (~76%),  
603 in particular by radiation (~43%) and precipitation (~16%). We note that the modular  
604 structure of PLASIM means that replacing the radiation scheme with, for example, a  
605 computationally fast semi-grey scheme (Frierson et al 2006) would be relatively  
606 straightforward. An efficient convective adjustment scheme (Betts and Miller 1986) is  
607 already available as an alternative to the default moisture budget scheme (Kuo 1965,  
608 1974).

609

### 610 **3.1 PLASIM-ENTS**

611 The choice was made to preserve the coupled PLASIM-ENTS model in its entirety.  
612 The slab ocean and sea ice modules are retained only to provide boundary conditions;  
613 their state variables are over-written with GOLDSTEIN and GOLDSTEINSEAICE  
614 outputs, effectively negating the very simple dynamics of these models. This  
615 simplifies the coupling because the energy and moisture flux calculations are already  
616 made within PLASIM. The changes needed to PLASIM with this approach are  
617 therefore kept to a minimum, consisting of prescribing the slab ocean with  
618 GOLDSTEIN distributions of sea surface temperature and the slab sea-ice with  
619 GOLDSTEINSEAICE distributions of sea-ice fractional coverage, height, surface  
620 temperature and albedo. Furthermore, although GENIE contains a stand-alone version  
621 of the land surface module ENTS, the decision was taken to leave the existing  
622 PLASIM-ENTS coupling in place. Future work may separate the PLASIM and ENTS  
623 modules. The primary motivation for this would be modularity. Notably GENIEified  
624 ENTS is coupled to the global carbon cycle (Lenton et al 2006) and has been enabled  
625 to simulate the effects of anthropogenic land use change (Holden et al 2013a).

626

### 627 **3.2 GOLDSTEIN**

628 No changes were made to GOLDSTEIN. Surface wind stress, net energy and net  
629 moisture fluxes are supplied from PLASIM, modified by sea ice where relevant. We

630 note that we use a PLASIM time step of 45 minutes and a GOLDSTEIN time step of  
631 12 hours, with coupling inputs averaged over the previous 16 PLASIM time steps (12  
632 hours.

633

### 634 3.3 GOLDSTEINSEAICE

635 In GENIE-1 the thermodynamics of GOLDSTEINSEAICE are calculated within the  
636 EMBM, and coupling to alternative model atmospheres is not possible with this  
637 model structure. To enable a PLASIM-GOLDSTEINSEAICE coupling we have  
638 developed a stand-alone sea-ice thermodynamics routine.

639

640 Time-averaged incoming energy fluxes and atmospheric boundary conditions  
641 are supplied to the new surface flux (ICE-SURFLUX) routine from PLASIM. Sea  
642 surface temperature and salinity, sea-ice height and fractional sea-ice coverage  
643 are provided from the previous GOLDSTEIN/SEAICE time step.

644

645 ICE-SURFLUX closely follows the formulation of Edwards and Marsh (2005),  
646 where it is described in some detail. We summarize the approach here. Sea ice is  
647 assumed to have no heat capacity, so that the heat flux exchanged with the  
648 atmosphere equals the heat flux through the ice, thereby defining the vertical  
649 temperature gradient across the ice. The temperature at the sea-ice base is  
650 assumed equal to the salinity-dependent freezing point of the surface ocean, so  
651 that the ice-surface temperature is the remaining unknown. Now we need to  
652 derive the net heat flux from the atmosphere. Incoming radiative fluxes are  
653 provided by PLASIM; outgoing radiative fluxes, and sensible and latent heat  
654 fluxes are dependent upon the surface temperature of the sea ice, together with  
655 atmospheric boundary conditions. These relationships together imply an ice-  
656 surface temperature (and the associated atmospheric heat flux) that balances the  
657 heat budget, which is solved for with a Newton-Raphson algorithm. The heat flux  
658 exchanged with the ocean is implied by the temperature differential between the  
659 sea-ice base (freezing point) and the surface ocean. The difference between the  
660 heat flux exchanged with the atmosphere and with the ocean is consumed by  
661 creating or melting ice.

662

Phil Holden 8/4/16 15:07

**Deleted:** ). The computational demands of the coupled model, simulating 75 years per day on a single node of a 256Gb 2.1GHz AMD 6172 CPU, are dominated by PLASIM (98%); the computational demands of PLASIM are dominated by diabatic processes (~76%), in particular by radiation (~43%) and precipitation (~16%).



671 The diagnosed energy and moisture fluxes are not passed to PLASIM. Instead, in  
672 order to achieve energy and moisture conservation, PLASIM transfer coefficients  
673 are used in the calculation of sensible heat and sublimation during the Newton-  
674 Raphson step. This ensures that net fluxes calculated in PLASIM (which use the  
675 sea-ice temperature and albedo derived in ICE-SURFLUX) will be consistent with  
676 those calculated in ICE-SURFLUX, but does not guarantee perfect conservation.  
677 Conservation errors arise through differential time-stepping (the averaging of  
678 non-linear flux terms over 16 PLASIM time steps) and also because PLASIM does  
679 not explicitly account for sea-ice leads; ICE-SURFLUX separately accounts for  
680 ocean and sea-ice in a partially covered gridcell, but PLASIM fluxes are derived  
681 from weighted average surface properties<sup>1</sup>. To evaluate the magnitude of the  
682 conservation errors, we consider all of the sea-ice covered grid cells at each time  
683 step across a year of the spun-up model. The energy conservation error across  
684 these 152,495 data points is  $0.1 \pm 1.0 \text{ Wm}^{-2}$  ( $1\sigma$ ). We note that the PLASIM  
685 atmosphere does not precisely conserve energy, as illustrated by Hoskins and  
686 Simmons (1975) for a similar dry dynamical core. The largest effect in PLASIM  
687 comes from the conversion from potential to kinetic energy. This conversion  
688 cannot be formulated in a conservative manner in the semi-spectral scheme  
689 since it involves triple products while the (Gaussian) grid only allows for the  
690 conservation of quadratic quantities. The top-of-atmosphere energy balance  
691 converges to  $-0.7 \text{ Wm}^{-2}$  in both the coupled and stand-alone versions of PLASIM,  
692 dominating over the conservation errors of ICE-SURFLUX.  
693  
694 Sea-ice growth rates are provided to GOLDSTEINSEICE, which derives updated  
695 sea-ice distributions, considering both thermodynamics and dynamics  
696 (advection and diffusion). The updated sea-ice distribution is provided to  
697 PLASIM and the associated freshwater exchange with the ocean is provided to  
698 GOLDSTEIN.

---

<sup>1</sup> A drift over the 2,000-year spin-up simulation is apparent in the 6<sup>th</sup> significant figure of global averaged salinity, likely also a consequence of the neglect of sea-ice leads in PLASIM and the differential timestepping. While this modest failure of moisture conservation is negligible for the physical model, it will be revisited

Phil Holden 8/4/16 15:07

Deleted: step gearing

Phil Holden 8/4/16 15:07

Formatted: Font: Cambria

Phil Holden 8/4/16 15:07

Deleted: because

Phil Holden 8/4/16 15:07

Formatted: Font: Cambria

Phil Holden 8/4/16 15:07

Formatted: Font: Cambria

Phil Holden 8/4/16 15:07

Deleted: a

Phil Holden 8/4/16 15:07

Deleted: model; the

Phil Holden 8/4/16 15:07

Formatted: Font: Cambria

Phil Holden 8/4/16 15:07

Formatted: Font: Cambria, 12 pt

703

#### 704 4. Tuning methodology

705 Our approach for the selection of a tuned set of parameter values was to retain  
 706 the existing tunings of models where possible (for exceptions see Section 4.1)  
 707 and to only consider the parametric uncertainty of GOLDSTEIN. The motivation  
 708 was that both PLASIM (Lunkeit et al 2007) and ENTS (Williamson et al 2006)  
 709 have already been tuned to reproduce observations when forced with  
 710 climatology<sup>2</sup>. In contrast, existing GOLDSTEIN tunings have been developed  
 711 within a coupled atmosphere-ocean model, usually the EMBM atmosphere. We  
 712 anticipated that a tuning of GOLDSTEIN that reproduces the main features of  
 713 global ocean circulation when coupled to climatologically tuned PLASIM-ENTS  
 714 would likely provide a good representation of observed climatology in general.

715

716 We performed a 50-member ensemble of 1,000-year preindustrial spin-up  
 717 simulations varying six GOLDSTEIN parameters, in the expectation that some  
 718 subset of ensemble members would produce reasonable climate states from  
 719 which we could select a tuned model. (Failure in this regard would have  
 720 necessitated the application of more sophisticated statistical techniques for  
 721 searching parameter input space).

722

#### 723 4.1 Ensemble design

724 Parameters from modules other than GOLDSTEIN were all fixed. However, some  
 725 were changed from their default values (or are recently introduced  
 726 parameterisations that are not associated with tuned defaults). These choices  
 727 were made on the basis of exploratory simulations:

728 vi) The uncertain effect of clouds on long wave radiation is controlled  
 729 through the dependence of cloud emissivity  $A$  on the mass absorption  
 730 factor  $k$  “aclwr”, following Slingo and Slingo (1991):

$$A = 1 - e^{-\beta k w}$$

for the carbon cycle coupling in order to ensure conservation of biogeochemical tracers.

<sup>2</sup> The diurnal cycle is switched off in these simulations, reflecting the default assumption for both the PLASIM and ENTS tunings.

Phil Holden 8/4/16 15:07  
 Deleted: besides

Phil Holden 8/4/16 15:07  
 Deleted: PLASIM parameter *acllwr* controls the

Phil Holden 8/4/16 15:07  
 Deleted: outgoing longwave

Phil Holden 8/4/16 15:07  
 Deleted: and

736  
737  
738  
739  
740  
741  
742  
743  
744  
745  
746  
747  
748  
749  
750  
751  
752  
753  
754  
755  
756  
757  
758  
759  
760  
761  
762  
763  
764  
765  
766

where  $\beta = 1.66$  is the diffusivity factor and  $W$  the cloud liquid water path. The mass absorption factor was found to exert the strongest control on surface air temperature of the 22 key model parameters considered in PLASIM-ENTS ensembles (Holden et al 2014). The value was increased from default  $k = 0.1$  to  $0.2 \text{ m}^2 \text{ g}^{-1}$ , estimated to yield a simulated global average surface air temperature of approximately  $14^\circ\text{C}$  in conjunction with parameter choices (ii) to (v) below.

vii) The PLASIM parameter *albseamax* defines the latitudinal variation of ocean albedo (Holden et al 2014),

$$\alpha_s = \alpha_{s0} + 0.5\alpha_{s1}[1 - \cos(2\varphi)]$$

where the ocean albedo  $\alpha_s$  is expressed in terms of latitude  $\varphi$ , the albedo at the equator  $\alpha_{s0} = 0.069$  and the parameter that controls latitudinal variability  $\alpha_{s1}$ . The calculated albedo is applied to both direct and scattered radiation. A high value ( $\alpha_{s1} = 0.4$ ) was favoured for *albseamax*, leading to cooler high latitude ocean and favouring increased Southern Ocean sea-ice and deep-water formation, which both tended to be too low with default parameters.

viii) Sea ice is transported through advection and Laplacian diffusion (Edwards and Marsh, 2005), the latter taking the place of a detailed representation of unresolved advection and rheological processes. Sea-ice diffusivity (*SID*) influences AABW formation by controlling the rate at which new ice is created, and hence the strength of brine rejection (Holden et al 2013b). A high value was favoured, again to strengthen deep-water formation, but values greater than  $15,000 \text{ m}^2 \text{ s}^{-1}$  were found to lead to numerical instabilities in this model and *SID* was fixed at this value.

ix) The standard PLASIM expression for the dependence of sea ice albedo  $\alpha_i$  on surface air temperature is used

$$\alpha_i = 0.5 - 0.025T_{air}$$

where  $T_{air}$  is the surface air temperature ( $^\circ\text{C}$ ). PLASIM restricts the maximum albedo to 0.7 ( $T_{air} \leq -8^\circ\text{C}$ ). In PLASIM-GENIE we additionally restrict the minimum albedo, to 0.5 ( $T_{air} \geq 0^\circ\text{C}$ ).

x) The PLASIM-ENTS dependency of photosynthesis on soil moisture is

Phil Holden 8/4/16 15:07  
**Formatted:** Indent: Left: 1.9 cm, No bullets or numbering

Phil Holden 8/4/16 15:07  
**Deleted:** *aclwv* parameter

Phil Holden 8/4/16 15:07  
**Deleted:** 0.1

Phil Holden 8/4/16 15:07  
**Deleted:**  $0.2 \text{ m}^2 \text{ g}^{-1}$ , a value

Phil Holden 8/4/16 15:07  
**Formatted:** Indent: Left: 1.9 cm, No bullets or numbering

Phil Holden 8/4/16 15:07  
**Deleted:** 0.4

Phil Holden 8/4/16 15:07  
**Deleted:** was used, but a minimum value  $\alpha_{min}$  was introduced, viz.

Phil Holden 8/4/16 15:07  
**Deleted:** Values of 0.5 and

Phil Holden 8/4/16 15:07  
**Deleted:** were applied for  $\alpha_{min}$  and  $\alpha_{max}$  respectively.

$$f_2(W_s) = \{(W_s/W_s^*) - q_{th}\} / \{0.75 - q_{th}\}$$

776 The parameter  $q_{th}$  ( $q_{thresh}$ ) was set to 0.1, allowing the development  
 777 of vegetation in semi-arid regions (Holden et al 2014).

778

779 The ensemble was generated using a 50x6 maximin latin hypercube design,  
 780 varying six GOLDSTEIN parameters, listed in Table 1, and varied over ranges,  
 781 considered to reflect the plausible range for each parameter (Holden et al 2013b  
 782 and references therein). The six varied parameters are isopycnal and diapycnal  
 783 diffusivities, a parameter  $OP1$  that controls the depth profile of diapycnal  
 784 diffusivity (see below), the frictional drag coefficient (GOLDSTEIN is based upon  
 785 the thermocline equations with the addition of a linear drag term in the  
 786 horizontal momentum equations, Edwards et al 1998), wind stress scaling (a  
 787 linear scaling of the surface wind-stress is applied to compensate for the energy  
 788 dissipated by frictional drag), and an Atlantic-Pacific moisture flux adjustment.

789

790 Diapycnal diffusivity is stratification-dependent (Oliver and Edwards, 2008),  
 791 given by

$$k_v = k_{v0} p_0(z)^\gamma \left( \frac{\Delta\rho_0(z)}{\Delta\rho(z)} \right)$$

792 where  $k_{v0}$  (reference diapycnal diffusivity) and  $\gamma$  ( $OP1$ ) are varied across the  
 793 ensemble (Table 1),  $p_0(z)$  is a reference profile (exponentially growing with  
 794 depth and equal to 1 at 2500m),  $\Delta\rho_0(z)$  a reference vertical density gradient  
 795 profile and  $\Delta\rho(z)$  the local simulated vertical density gradient.

796

797 Two ensemble parameters merit particular discussion here:

798

#### 799 4.1.1 APM

800 APM is a flux adjustment that transports moisture from the Atlantic to the Pacific,  
 801 originally developed for the EMBM coupling (Edwards and Marsh, 2005). The  
 802 default flux adjustment (0.32Sv) is subdivided into three latitude bands  
 803 reflecting the observed Atlantic-Pacific moisture transport (Oort, 1983): -0.03Sv  
 804 south of 20°S, 0.17Sv in the tropical zone 20°S to 24°N, and 0.18Sv north of 24°N.  
 805 Exploratory simulations suggested that PLASIM-GENIE would likely require a

Phil Holden 8/4/16 15:07  
**Formatted:** Indent: Left: 1.9 cm, No bullets or numbering

Phil Holden 8/4/16 15:07  
**Deleted:** the

Phil Holden 8/4/16 15:07  
**Deleted:** tabulated

Phil Holden 8/4/16 15:07  
**Deleted:** . The

Phil Holden 8/4/16 15:07  
**Deleted:** are

Phil Holden 8/4/16 15:07  
**Deleted:** Two parameters merit particular discussion here:

Phil Holden 8/4/16 15:07  
**Deleted:** correction

Phil Holden 8/4/16 15:07  
**Deleted:** correction

814 moisture flux adjustment and *APM* was introduced as an ensemble variable. *APM*  
815 is varied across ensemble members by a linear scaling preserving the ratio of  
816 fluxes between latitude bands.

817

818 An exploratory simulation with a flux adjustment of 0.32Sv was performed and  
819 integrated net input freshwater fluxes (precipitation, evaporation, runoff and the  
820 flux adjustment) were diagnosed for the Arctic/Atlantic and the Pacific. In both  
821 basins, grid cells north of 32°S were included, following the observational  
822 estimates of Talley (2008). Values of -0.5Sv and +0.1Sv respectively were  
823 diagnosed, compared to observations of -0.28±0.04 and +0.04 ± 0.09Sv (Talley  
824 2008). Informed by this result, we allowed *APM* to vary in the range 0 to 0.32Sv.

825

826 PLASIM has also been coupled to the UVic Earth system model, creating the  
827 OSUVic model (Schmittner et al, 2010). The most significant difference between  
828 PLASIM-GENIE and USOVic is the differing complexity of the ocean models; USO-  
829 Vic incorporates the more complex primitive-equation Modular Ocean Model  
830 (MOM) version 2.2 (Pacanowski 1995) at a horizontal resolution of 1.8° x 3.6°.  
831 The primitive equations include momentum advection terms neglected in our  
832 system. At T21 atmospheric resolution, the integrated Atlantic surface moisture  
833 balance simulated by OSUVic (-0.33Sv) is in good agreement with observations  
834 without any flux adjustment. However, OSUVic nevertheless simulates a weak  
835 (9Sv) Atlantic overturning circulation at T21 resolution. This was attributed in  
836 part to errors in the latitudinal distribution of the simulated moisture flux, which  
837 create low surface ocean salinities at high latitudes in the Atlantic (balanced by  
838 high salinity at low latitudes). We note that an exploratory PLASIM-GENIE  
839 simulation with a *uniformly* distributed 0.32Sv moisture flux adjustment also  
840 exhibited low Atlantic salinity at high latitudes and weak overturning.

841

#### 842 4.1.2 SCF

843 *SCF* scales the surface wind stresses that are applied to GOLDSTEIN. The scaling  
844 is needed because the frictional-geostrophic ocean dissipates wind energy so  
845 that increased surface wind strengths are required to compensate and drive a  
846 reasonable circulation. The conventional ensemble range for the *SCF* parameter

Phil Holden 8/4/16 15:07

**Deleted:** correction

Phil Holden 8/4/16 15:07

**Deleted:** across the

Phil Holden 8/4/16 15:07

**Deleted:** correction

Phil Holden 8/4/16 15:07

**Deleted:** correction

Phil Holden 8/4/16 15:07

**Deleted:** At T21 resolution

Phil Holden 8/4/16 15:07

**Deleted:** correction

Phil Holden 8/4/16 15:07

**Deleted:** correction

Phil Holden 8/4/16 15:07

**Formatted:** Font color: Auto

854 in GENIE-1 (forced by observed climatological wind stress) is 1 to 3 (Edwards  
855 and Marsh, 2005).

856

857 In the OSUVic model (Schmittner et al 2010), the weak overturning circulation at  
858 T21 resolution discussed in Section 4.1.1 was, in addition to errors in the surface  
859 salinity distribution, partly attributed to low zonal wind-stress in the Southern  
860 Ocean, likely due to inadequate meridional resolution (c.f. Held and Phillipps,  
861 1993). In anticipation of systematically understated zonal wind stress in our T21  
862 coupling, we here allowed *SCF* to vary in the range 2 to 4.

863

## 864 **4.2 Ensemble outputs**

865 Thirty-seven of the 50 ensemble members successfully completed the 1,000-year  
866 preindustrial spin up simulations. These simulations exhibited a global average  
867 surface air temperature of  $12.1 \pm 1.2^\circ\text{C}$  ( $1\sigma$ ). Simulation-failure was invariably  
868 associated with low frictional drag (high *ADRAG*); low frictional drag leads to  
869 unrealistically strong flow near the Equator and topographic features (Edwards  
870 and Marsh, 2005). Three successfully completed simulations (with inverse  
871 frictional drag 4.01, 3.21 and 3.98 days<sup>-1</sup>) were excluded from the ensemble on  
872 account of unreasonably strong Pacific overturning (277, -174 and 633Sv  
873 respectively). We briefly summarise some of the characteristics of the remaining  
874 thirty-four simulations in terms of their response to *APM*, *SCF* and *ADRAG*, the  
875 three parameters that dominate the ensemble variability.

876

### 877 **4.2.1 APM**

878 The Atlantic overturning cell collapsed in all 20 simulations with *APM* less than  
879 0.16Sv. It collapsed in only five of the 14 simulations with *APM* greater than  
880 0.16Sv.

881

882 A regression of ensemble outputs suggests that the observed integrated Atlantic  
883 freshwater balance (correlation -0.88) is best reproduced for *APM* of  
884 approximately 0.13Sv, while the integrated Pacific freshwater balance  
885 (correlation +0.57) is best reproduced for *APM* of approximately 0.28Sv. Values

Phil Holden 8/4/16 15:07

Formatted: Font color: Auto

886 between these limits ( $\sim 0.13$  to  $0.28\text{Sv}$ ) are therefore favoured to optimise the  
887 surface ocean inter-basin salinity distribution.

888

889 It is worth noting that these conclusions only pertain to the specific model setup  
890 considered (i.e. the vector of all *fixed* parameters). We cannot rule out the  
891 possibility that alternative model parameterisations can reproduce observed  
892 salinity and circulation fields without a moisture flux adjustment.

893

894 **4.2.2 SCF and ADRAG:** Wind stress scaling and inverse frictional drag affect the  
895 simulations in similar ways, as expected because the role of wind-stress scaling  
896 is to compensate for frictional dissipation. Many clear relationships between  
897 these parameters and simulated outputs are apparent, for instance high values of  
898 either tend to strengthen overturning circulation and decrease sea-ice coverage  
899 in both hemispheres. It is interesting to note a strong negative correlation ( $-0.62$ )  
900 between *ADRAG* and the integrated surface Pacific freshwater flux, opposing a  
901 positive correlation ( $+0.77$ ) with the integrated freshwater flux of the Indian  
902 Ocean. (Similar, though weaker, relationships exist with *SCF*).

903

#### 904 **4.3 Selection of a 'subjectively' tuned parameter set**

905 Three of the 37 completed 1,000-year simulations have already been ruled out  
906 for unreasonably strong Pacific overturning and a further twenty-five because  
907 the Atlantic overturning circulation had collapsed. Two further simulations were  
908 ruled out for unacceptably low (and still cooling) global surface air temperature  
909 ( $<10^\circ\text{C}$ ) and two for an excessively evaporative Atlantic basin ( $\sim 0.5\text{Sv}$ , forced by  
910 *APM*  $\sim 0.3\text{Sv}$ ). The remaining five simulations were spun on for an additional  
911 1,000 years. After this spin on, two of these simulations were ruled out under a  
912 stricter global surface air temperature constraint (requiring  $>12^\circ\text{C}$ ), a third  
913 simulation did not exhibit penetration of Antarctic Bottom Water into the  
914 Atlantic and a fourth simulation displayed a positive Pacific overturning cell that  
915 penetrated to the ocean floor north of  $15^\circ\text{N}$ . The remaining simulation was  
916 clearly preferable on the basis of these simple large-scale constraints, testing for

Phil Holden 8/4/16 15:07

Deleted: correction

918 reasonable surface-ocean forcing and circulation. This ‘subjective’ parameter set  
919 (see Table 1) is therefore taken as our preferred tuning<sup>3</sup>.

920

## 921 **5.0 Simulated climate of the subjective tuning**

922 The simulated climate metrics of the subjective tuning are global average surface  
923 air temperature 12.9°C, surface Atlantic freshwater balance -0.34Sv (including  
924 the -0.21Sv moisture flux [adjustment](#)), maximum Atlantic overturning (below  
925 500m) 15.5Sv, minimum Atlantic overturning -3.4Sv, and maximum Pacific  
926 overturning 8.8Sv (restricted to high latitudes and intermediate depths, see  
927 Figure 6). We now evaluate the climate in some detail.

928

929 Table 2 compares the subjectively tuned PLASIM-ENTS preindustrial global  
930 energy balance against a range of observationally constrained (present day)  
931 estimates presented in Trenberth et al (2009). Simulated fluxes are generally  
932 within the ranges of these estimates besides reflecting the simulated cold bias  
933 that is most clearly apparent in OLR (and only partially attributable to  
934 anthropogenic forcing). Although within ranges, these data suggest that too little  
935 solar radiation is absorbed within the atmosphere and too much is reflected by  
936 the surface (likely due to the high ocean albedo, Section 4.1).

937

938 Table 3 compares the simulated surface ocean net moisture fluxes in each basin  
939 with the estimates of Talley (2008). The good agreement in the Atlantic is  
940 imposed by the moisture flux [adjustment](#). We emphasise that the requirement  
941 for a flux [adjustment](#) in this parameterisation does not necessarily indicate an  
942 inherent structural weakness in the model, pending a full exploration of  
943 parameter-space (c.f. Williamson et al 2015). The largest disagreement between  
944 these observations and the subjective tuning is the moisture flux differential  
945 between the Indian and Pacific Oceans. The global aggregates of precipitation,

Phil Holden 8/4/16 15:07

~~Deleted:~~ correction

Phil Holden 8/4/16 15:07

~~Deleted:~~ correction

Phil Holden 8/4/16 15:07

~~Deleted:~~ correction

---

<sup>3</sup> We note that after the tuning ensemble was performed, the “surfstep” PLASIM subroutine was moved to the start of the diabatic time step (in the stand-alone model, PLASIM surface conditions are updated after the calculation of diabatic processes). This change was made so that boundary conditions are immediately



949 evaporation and runoff are in good agreement with the observationally  
950 constrained estimates of Trenberth et al (2007), with a modest low bias that is  
951 consistent with the simulated cold bias.

952

953 Figures 2 to 4 compare a selection of PLASIM-GENIE outputs against  
954 NCEP/NCAR reanalysis fields (Kalnay et al 1996). In each case we compare fifty-  
955 year PLASIM-GENIE averages of southern summer (JJA) and northern summer  
956 (DJF) with the corresponding long-term means (1981-2010) of the reanalysis  
957 data. The plotted outputs were chosen to highlight feedbacks that are neglected  
958 by the EMBM, viz. 3D dynamical atmospheric transport, providing greatly  
959 improved precipitation fields and dynamic surface winds (an imposed forcing in  
960 GENIE-1), and interactive clouds (also an imposed forcing field in GENIE-1,  
961 comprising a spatiotemporal cloud albedo field and uniform OLR adjustment.)

962

963 Surface air temperature and precipitation fields are plotted in Figure 2. The cold  
964 bias of the subjective tuning is especially apparent in the high Arctic winter.  
965 Despite the global cold bias, surface air temperatures are warm-biased over the  
966 Southern Ocean, consistent with an underestimation of southern sea-ice  
967 coverage that was apparent over the entire ensemble. PLASIM precipitation  
968 fields are reasonable given our low resolution. Distinct arid regions are captured,  
969 as is the seasonal migration of the Inter-Tropical Convergence Zone and  
970 associated monsoon systems.

971

972 Figure 3 compares the surface wind fields of the subjective tuning with 10m  
973 reanalysis winds. The simulated spatiotemporal distributions are in good  
974 agreement with reanalysis, although Antarctic circumpolar wind speed is  
975 somewhat understated and too northerly (c.f. Schmittner et al 2010). We note  
976 that simulated wind speeds are at the 0.983 sigma pressure level, typically  
977 ~136m above the surface, so that boundary layer damping is weaker than the  
978 10m reanalysis winds. Therefore we expect greater wind speeds in the PLASIM-

---

updated after a call to GOLDSTEIN. Differences in simulated outputs were not distinguishable from internal variability.

Phil Holden 8/4/16 15:07

**Deleted:** The selected variables were chosen to highlight feedbacks neglected by the EMBM.

Phil Holden 8/4/16 15:07

**Deleted:** monthly

Phil Holden 8/4/16 15:07

**Deleted:** July and January,

Phil Holden 8/4/16 15:07

**Deleted:** .

... [1]

Phil Holden 8/4/16 15:07

**Deleted:** Precipitation over the eastern Pacific Ocean is generally understated, while it is overstated over the eastern Atlantic Ocean, consistent with the need for an Atlantic-Pacific moisture-flux correction to generate reasonable salinity distributions and an Atlantic overturning circulation.

993 GENIE plots, as is generally the case. Our focus here is on the wind-stress  
994 coupling and the tuned ocean state. The 3D atmospheric circulation is also  
995 reasonable. To illustrate, the simulated Southern/Northern hemisphere winter  
996 zonal wind jets (~44/43 ms<sup>-1</sup>, 35°S/35°N, 150mbar) compare to reanalysis data  
997 (~41/44 ms<sup>-1</sup>, 30°S/30°N, 200mbar),

Phil Holden 8/4/16 15:07

Formatted: Font color: Auto

999 Figure 4 compares incoming solar and thermal radiation fields with the  
1000 reanalysis data. These fields are also chosen to reflect dynamics that are absent  
1001 from GENIE-1, which applies prescribed planetary albedo fields and a globally  
1002 uniform OLR adjustment to represent the effect of clouds on the radiation  
1003 balance. Although the representation of clouds in PLASIM is of low complexity,  
1004 the ability of the model to represent dynamic cloud feedbacks represents a  
1005 substantial improvement upon GENIE-1.

1006

1007 The outputs plotted in Figures 3 and 4 were chosen to focus on dynamics that  
1008 are entirely absent from GENIE-1: interactive winds and interactive clouds.  
1009 While the inclusion of these dynamics is not expected to improve the simulated  
1010 climatology (i.e. when compared to simulations that are forced with  
1011 climatological fields), their inclusion represents a substantial upgrade through  
1012 the capture of important Earth system feedbacks neglected in GENIE-1.

Phil Holden 8/4/16 15:07

Deleted: PLASIM coupling improves

1014 An important example of substantial improvement over the climatology of  
1015 GENIE-1 is atmospheric moisture transport, previously touched upon in the  
1016 context of Figure 2. Figure 5 compares PLASIM-GENIE vegetative carbon (5a)  
1017 and GENIE-1 vegetation carbon (5b, data reproduced from Holden et al, 2013a,  
1018 Fig 1a) and highlights various aspects of the improved moisture transport. In

Phil Holden 8/4/16 15:07

Deleted: 5a) with respect to GENIE-1.

1019 GENIE-1, deserts are poorly resolved (too moist) and boreal forest does not  
1020 penetrate far into the continental interior of Eurasia, (too dry); these are both

Phil Holden 8/4/16 15:07

Deleted: ,

1021 shortcomings that arise from diffusive moisture transport (Lenton et al 2006).  
1022 Although the deserts of the Southern hemisphere are not well resolved in either  
1023 model, the larger deserts of the Northern hemisphere are distinct in PLASIM-  
1024 GENIE, while simulated boreal forest penetrates the Eurasian interior. Global  
1025 terrestrial carbon storage in the subjective tuning of PLASIM-GENIE is 604GTC

1029 (vegetation) and 1,971GTC (soil). These compare to 491-574 GTC and 1,367-  
1030 1,416GTC respectively in GENIE-1 (Lenton et al 2006). The significantly higher  
1031 soil carbon values in PLASIM-GENIE primarily reflect the increased area of  
1032 Eurasian boreal forest, where soil carbon is respired slowly due to the low  
1033 temperatures. The global terrestrial carbon pools are consistent with ranges of  
1034 460-660GTC (vegetation) and 850-2400GTC (soil) derived from a range of  
1035 observational and modelling studies and summarised in Bondeau et al (2007).

1036

1037 Budyko's (1974) framework of climate analysis is based on the climate mean  
1038 dryness ratio  $D$  or aridity index (mean energy supply or net radiation  $N$  to mean  
1039 water supply or precipitation  $P$ ). It provides quantitative geobotanically relevant  
1040 thresholds for land surface climate regimes that are related to vegetation  
1041 structures (Fig. 6c): Tundra,  $D < 1/3$ , and forests,  $1/3 < D < 1$ , are energy limited  
1042 ( $D < 1$ ), because available energy  $N$  is low, so that runoff exceeds evaporation for  
1043 given precipitation,  $E \sim N$ . Steppe and savanna,  $1 < D < 2$ ; semi-desert,  $2 < D < 3$ ;  
1044 and desert  $3 > D$ , are water-limited climates ( $D > 1$ ), where the available energy  
1045 is so high that water supplied by precipitation evaporates, which then exceeds  
1046 runoff,  $E - P$ . This analysis highlights the Tibetan Plateau and North American  
1047 Arctic climates and demonstrates consistency with the simulated vegetation  
1048 carbon (Fig. 6a). The similarity with ERA-interim based analysis (Cai et al 2014,  
1049 Fig 1a) is notable. Similarly, a bucket model interpretation of the land surface  
1050 climate (Fraedrich et al 2015) is possible using the soil moisture fraction,  
1051  $S = s/s^* = E/N$ , and is plotted in Fig. 5d.

1052

1053 Sea-ice distributions (not illustrated) exhibit a systematic bias towards low  
1054 southern sea-ice area across the ensemble, with an annual average of 2.8 million  
1055 km<sup>2</sup> in the subjective tuning; this compares to observational estimates of 11.5  
1056 million km<sup>2</sup> (Cavalieri et al 2003). Surface air temperature over the southern  
1057 ocean is warm biased with respect to the reanalysis data, despite a modest cold  
1058 bias in the global temperature (Figure 2). While this may in part be a  
1059 consequence of reduced sea-ice (through the albedo feedback), the continued  
1060 presence of the warm bias in southern summer suggests the possibility that the  
1061 bias arises in the atmosphere. The decision to control the global temperature

Phil Holden 8/4/16 15:07

Deleted: 5c

Phil Holden 8/4/16 15:07

Deleted: 5a

1064 with *acllwr* (Section 4.1) preferentially warms cloudy regions and may have  
1065 contributed. Indeed, simulated downward thermal radiation exhibits a  
1066 significant bias over the Southern Ocean (Figure 4). A thorough investigation of  
1067 the source of this bias is beyond the scope of this study, requiring consideration  
1068 of uncertainties in atmospheric and ocean energy transport, and in solar and  
1069 thermal radiative transfer, considering clouds, water vapour, and surface  
1070 processes.

1071

1072 Figure 6 illustrates the simulated ocean state. Plots The upper four panels reflect  
1073 the constraints imposed upon the subjective parameter set and require little  
1074 further discussion. It is worth emphasising again that the simulation of realistic  
1075 salinity fields and ocean circulation required an Atlantic-Pacific moisture flux  
1076 adjustment in this paramaterisation (Sections 4.1.1 and 4.2.1). The lower panel  
1077 of Figure 6 illustrates wind-driven AMOC variability, behaviour that is absent  
1078 from GENIE-1 (Sarojini et al 2011), because it is forced with annual averaged  
1079 climatological winds; the maximum Atlantic overturning circulation is plotted  
1080 through an arbitrary year (year 100 of a spin on simulation), together with the  
1081 100-year mean and standard deviation.

1082

## 1083 **6.0 Summary and conclusions**

1084

1085 We have presented a new intermediate complexity AOGCM PLASIM-GENIE,  
1086 which reproduces the main features of the climate system well and represents a  
1087 substantial upgrade to GENIE-1 through the representation of important  
1088 atmospheric dynamical feedbacks that are absent in an EMBM. PLASIM-GENIE  
1089 has been developed to join the limited number of intermediate complexity  
1090 models with primitive equation atmospheric dynamics. It supersedes an earlier  
1091 coupling with the IGCM ('GENIE-2'), which was contaminated with spurious  
1092 numerically generated features, limiting its usefulness.

1093

1094 The simple 'subjective' tuning approach applied here considered only six ocean  
1095 parameters, seeking a reasonable ocean circulation when coupled to PLASIM-  
1096 ENTS (both PLASIM and ENTS have previously been tuned with climatological

Phil Holden 8/4/16 15:07

**Deleted:** These plots each

1098 forcing). This limited tuning approach required approximately 2 CPU years,  
1099 demanding but readily tractable, representing approximately two weeks of  
1100 computation on 50 cluster nodes.

1101

1102 A reasonable ocean circulation state and salinity distribution required the  
1103 application of an Atlantic-Pacific moisture flux adjustment. We do not rule out  
1104 the possibility that a full investigation of PLASIM-GENIE parametric uncertainty  
1105 could generate a plausible ocean circulation without a flux adjustment, and may  
1106 additionally resolve the understated southern sea ice. However, a  
1107 comprehensive tuning will demand the application of more complex statistical  
1108 approaches designed to deal with computationally demanding simulators. For  
1109 instance, the use of emulators to inform a sequential ensemble design process  
1110 has been demonstrated to yield a ~100-fold reduction in computational demand  
1111 (Holden et al 2015).

1112

### 1113 7.0 Code availability

1114 The code base is stored on a password-protected SVN server  
1115 [https://svn.ggy.bris.ac.uk/subversion/genie/branches/PLASIM\\_coupling](https://svn.ggy.bris.ac.uk/subversion/genie/branches/PLASIM_coupling)

1116

1117 Contact the authors for the password. The model is under continuous development;  
1118 see SVN revision 9657 for traceability.

1119

1120 We recommend setting up a root directory (e.g. PLASIM-GENIE) containing the  
1121 subdirectories `genie_output` and `genie`, the latter containing the directory structure  
1122 downloaded from the SVN repository.

1123

1124 In addition to the source code, PLASIM-GENIE makes use of several applications  
1125 and packages. You must have the following list of prerequisites installed on your  
1126 computer before you can run the model: Python, Perl, GNU make, the BASH shell, a  
1127 C++ compiler, a Fortran compiler that supports Fortran90, and NetCDF libraries  
1128 (compiled on the same computer using the same compilers that you will use to  
1129 compile PLASIM-GENIE).

1130

Phil Holden 8/4/16 15:07

**Deleted:** correction

Phil Holden 8/4/16 15:07

**Deleted:** correction

Phil Holden 8/4/16 15:07

**Deleted:** provided as supplementary material.

Phil Holden 8/4/16 15:07

**Deleted:** . The subdirectory `genie` will be the code base that you download from the supplementary material. This code base contains the entire GENIE model, except that input data files required for modules other than `pl_go_gs` have been removed in order to satisfy the data limits for GMD supplementary material. The full code base is available on request from the authors.

Phil Holden 8/4/16 15:07

**Formatted:** English (US)

1144 Before you compile the model you must provide information about i) where you have  
1145 installed the source code, ii) which compilers you are using, and iii) the location of  
1146 the netCDF libraries that you have created; this is achieved by editing the files  
1147 **user.mak** and **user.sh** in the directory genie-main. Comments in those files explain  
1148 which lines need to be edited.

1149

1150 A configuration file contains all the information required to specify a simulation.

1151 The code base includes a configuration file, to perform a 1,000-year spin-up with the

1152 subjective parameter set, “genie/genie-main/configs/pl\_go\_gs\_GMD.xml”. This

1153 configuration file has been fully commented for traceability to this model description

1154 paper and to explain how to generalize to other model realisations. To run this

1155 simulation, enter the genie/genie-main directory and type:

1156

1157 make cleanall

1158 ./genie.job -f configs/pl\_go\_gs\_GMD.xml

1159

1160 The outputs of this simulation will be directed to genie\_output/GMD\_subjective.

1161

1162 Acknowledgements. The work of Kirk, Lunkeit and Zhu was supported through

1163 the Cluster of Excellence 'CliSAP' (EXC177), Universität Hamburg, funded

1164 through the German Science Foundation (DFG).

1165

## 1166 **References**

1167

1168 Annan, J.D., Lunt D.J., Hargreaves, J.C. and Valdes, P.J.: Parameter estimation in an

1169 atmospheric GCM using the Ensemble Kalman Filter. Nonlinear Processes in

1170 Geophysics, European Geosciences Union (EGU), 12, 363-371, doi:1607-

1171 7946/npq/2005- 12-363, 2005.

1172

1173 Betts, A.K. and Miller, M.J.: A new convective adjustment scheme. Part II: Single

1174 column tests using GATE wave, BOMEX, ATEX and arctic air-mass data sets.

1175 Quart. J. R. Met. Soc., 112, 693–709, 1986.

1176

Phil Holden 8/4/16 15:07

**Deleted:** needed

Phil Holden 8/4/16 15:07

**Deleted:**

Phil Holden 8/4/16 15:07

**Deleted:** .

Phil Holden 8/4/16 15:07

**Formatted:** Font:+Theme Body, English (UK)

Phil Holden 8/4/16 15:07

**Deleted:** output

1181 Bondeau, A., Smith, P. C., Zaehle, S., Schaphoff, S., Lucht, W., Cramer, W., Gerten,  
1182 D., Lotze-Campen, H., Müller, C., Reichstein, M., and Smith, B.: Modelling the role  
1183 of agriculture for the 20th century global terrestrial carbon balance, Glob.  
1184 Change Biol., 13, 679–706, doi:10.1111/j.1365- 2486.2006.01305.x, 2007.

1185

1186 Budyko, M. : Climate and Life. Vol. 18, Academic Press, 508 pp, 1974.

1187

1188 Cai, D., Fraedrich, K., Sielmann, F., Guan, Y., Guo, S., Zhang, L. and Zhu, X.: Climate  
1189 and vegetation: an ERA-interim and GIMMS NVDI analysis, Journal of Climate, 27,  
1190 5111-5118, doi: 10.1175/JCLI-D-13-00674.1, 2014

1191

1192 Cavalieri, D. J., Parkinson, C. L., and Yinnikov, K. Y.: 30-year satellite record  
1193 reveals contrasting Arctic and Antarctic decadal sea-ice variability, Geophys. Res.  
1194 Lett., 30, 1970, doi:10.1029/2003GL018031, 2003.

1195

1196 Dahms, E., Borth, H., Lunkeit, F., and Fraedrich, K.: ITCZ splitting and the  
1197 influence of large-scale eddy fields on the Tropical mean state, J. Meteorol. Soc.  
1198 Jpn., 89, 399–411, doi:10.2151/jmsj.2011-501, 2011.

1199

1200 Edwards, N.R. and Marsh, R.: Uncertainties due to transport-parameter sensitivity in  
1201 an efficient 3-D ocean-climate model, Climate Dynamics, 24, 415-433, doi:  
1202 10.1007/s00382-004-0508-8, 2005.

1203

1204 [Edwards, N.R., Willmott, A.J. and Killworth, P.D.: On the role of topography and](#)  
1205 [wind stress on the stability of the thermohaline circulation. J. Physical Oceanography,](#)  
1206 [28, 756-778, 1998.](#)

1207

1208 Fanning, A. F. and Weaver, A. J.: An atmospheric energy-moisture balance model:  
1209 climatology, interpentadal climate change, and coupling to an ocean general  
1210 circulation model, Journal of Geophysical Research, 101, 15111–15128,  
1211 doi:10.1029/96JD01017, 1996.

1212

Phil Holden 8/4/16 15:07

Deleted: Müller

1214 de Forster, P.M., Blackburn, M., Glover, R. and Shine, K.P.: An examination of  
1215 climate sensitivity for idealised climate change experiments in an intermediate  
1216 general circulation model. *Climate Dynamics*, 16, 833–849, doi:  
1217 10.1007/s003820000083, 2000.  
1218  
1219 Fraedrich, K., Kirk, E., Luksch, U. and Lunkeit, F.: The portable university model of  
1220 the atmosphere (PUMA): Storm track dynamics and low-frequency variability,  
1221 *Meteorologische Zeitschrift*, 14, 735-745, doi: 10.1127/0941-2948/2005/0074, 2005.  
1222  
1223 Fraedrich, K. and Lunkeit, F.: Diagnosing the entropy budget of a climate model,  
1224 *Tellus A*, 60, 921–931, doi:10.1111/j.1600- 0870.2008.00338.x, 2008, 2008.  
1225  
1226 Fraedrich, K.: A suite of user-friendly climate models: Hysteresis experiments,  
1227 *The European Physical Journal Plus*, 127, 10.1140/epjp/i2012-12053-7, 2012  
1228  
1229 Fraedrich, K., Sielmann, F., Cai, D., and Zhu, X.: Climate dynamics on watershed  
1230 scale: along the rainfall-runoff chain. In: *The Fluid Dynamics of Climate*,  
1231 International Centre for Mechanical Sciences (CISM), Springer Verlag, [183-209](#),  
1232 [2016](#).  
1233  
1234 [Frierson, D.M.W., Held, I.M. and Zurita-Gotor, P.: A gray-radiation aquaplanet](#)  
1235 [moist GCM. Part I. Static stability and eddy scale, \*J. Atmos. Sci.\*, 63, 2548-2566,](#)  
1236 [2006](#)  
1237  
1238 Held, I.M. and Phillipps, P.J.: Sensitivity of the eddy momentum flux to meridional  
1239 resolution in atmospheric GCMs, *Journal of Climate*, 6, 499-507, 1995.  
1240  
1241 Holden, P.B. and Edwards, N.R.: Dimensionally reduced emulation of an AOGCM  
1242 for application to integrated assessment modelling, *Geophysical Research*  
1243 *Letters*, 37, L21707, doi:10.1029/2010GL045137, 2010.  
1244  
1245 Holden, P.B., Edwards, N.R., Oliver, K.I.C, Lenton, T.M. and Wilkinson R.D.: A  
1246 probabilistic calibration of climate sensitivity and terrestrial carbon storage in

Phil Holden 8/4/16 15:07

Deleted: 2015



1248 GENIE-1, *Climate Dynamics*, 35, 785-908, doi: 10.1007/s00382-009-0630-8,  
1249 2010.  
1250  
1251 Holden, P.B., Edwards, N.R., Gerten, D. and Schaphoff, S.: A model-based constraint  
1252 on CO<sub>2</sub> fertilisation, *Biogeosciences*, 10, 339-355, doi:10.5194/bg-10-339-2013,  
1253 2013a.  
1254  
1255 Holden, P.B., Edwards, N.R., Müller, S.A., Oliver, K.I.C., Death, R.M. and Ridgwell,  
1256 A.: Controls on the spatial distribution of  $\delta^{13}\text{C}$ , *Biogeosciences*, 10, 1815-1833,  
1257 doi:10.5194/bg-10-1815-2013, 2013b.  
1258  
1259 Holden, P.B., Edwards, N.R., Garthwaite, P.H., Fraedrich, K., Lunkeit, F., Kirk, E.,  
1260 Labriet, M., Kanudia, A. and Babonneau, F.: PLASIM-ENTSem v1.0: a spatio-  
1261 temporal emulator of future climate change for impacts assessment, *Geosci.*  
1262 *Model Dev.*, 7, 433-451, doi:10.5194/gmd-7-433-2014, 2014.  
1263  
1264 Holden, P.B., Edwards, N.R., Hensman, J. and Wilkinson, R.D.: ABC for climate:  
1265 dealing with expensive simulators, In S. A. Sisson, Y. Fan, and M. Beaumont eds.  
1266 *Approximate Bayesian Computation: Likelihood-Free Methods for Complex Models*,  
1267 Chapman and Hall, in press.  
1268  
1269 [Hoskins, B.J. and Simmons, A.J.: A multi-layer spectral model and the semi-](#)  
1270 [implicit method, \*Quart. J. R. Met. Soc.\*, 101, 637-655, doi:10.1002/](#)  
1271 [qj.49710142918, 1975.](#)  
1272  
1273 Kalnay, E., Kanamitsu, M., Kistler, R., Collins, W., Deaven, D., Gandin, L., Iredell, M.,  
1274 Saha, S., White, G., Woollen, J., Zhu, Y., Leetmaa, A., Reynolds, R., Chelliah, M.,  
1275 Ebisuzaki, W., Higgins, W., Janowiak, J., Mo, K. C., Ropelewski, C., Wang, J., Jenne,  
1276 R., and Joseph, D.: The NCEP/NCAR 40-Year Reanalysis Project. *Bull. Amer.*  
1277 *Meteor. Soc.*, 77, 437-471, 1996.  
1278  
1279 Labriet, M., Joshi, S.R., Vielle, M., Holden, P.B., Edwards, N.R., Kanudia, A.,  
1280 Loulou, R. and Babonneau, F.: Worldwide impacts of climate change on energy for

Phil Holden 8/4/16 15:07  
Formatted: Font:Not Italic

1281 heating and cooling, *Mitigation and Adaptation Strategies for Global Change*, doi:  
1282 10.1007/s11027-013-9522-7, 2013.

1283

1284 Lenton, T.M., Williamson, M.S., Edwards, N.R., Marsh, R., Price, A.R., Ridgwell, A.J.,  
1285 Shepherd, J.G., Cox, S.J. and The GENIE team: Millennial timescale carbon cycle  
1286 and climate change in an Efficient Earth system model, *Climate Dynamics*, 26,  
1287 687-711, doi: 10.1007/s00382-006-0109-9, 2006.

1288

1289 Lenton, T. M., Aksenov, Y., Cox, S.J., Hargreaves, J.C., Marsh, R., Price, A.R., Lunt,  
1290 D.J., Annan, J.D., Cooper-Chadwick, T., Edwards, N.R., S. Goswami, S., Livina,  
1291 V.N., P. J. Valdes, P.J., Yool, A., Harris, P.P., Jiao, Z., Payne, A.J., Rutt, I.C.,  
1292 Shepherd, J.G. Williams, G., Williamson, M.S.: Effects of atmospheric dynamics and  
1293 ocean resolution on bi-stability of the thermohaline circulation examined using the  
1294 Grid Enabled Integrated Earth system modelling (GENIE) framework, *Climate*  
1295 *Dynamics*, 29, 591–613, doi:10.1007/s00382-007-0254-9, 2007.

1296

1297 Lunkeit, F., Böttinger, M., Fraedrich, K., Jansen, H., Kirk, E., Kleidon, A. and Luksch  
1298 U.: Planet Simulator Reference Manual Version 15.0,  
1299 <http://epic.awi.de/29588/1/Lun2007d.pdf>, 2007.

1300

1301 [Kuo, H. L.: On formation and intensification of tropical cyclones through latent heat](#)  
1302 [release by cumulus convection. \*J. Atmos. Sci.\*, 22, 40–63, 1965.](#)

1303

1304 [Kuo, H. L.: Further studies of the parameterization of the influence of cumulus](#)  
1305 [convection on large-scale flow. \*J. Atmos. Sci.\*, 31, 1232–1240, 1974.](#)

1306

1307 Marsh, R., Müller, S.A., Yool, A. and Edwards, N.R.: Incorporation of the C-  
1308 GOLDSTEIN efficient climate model into the GENIE framework: “eb-go-gs”  
1309 configurations of GENIE, *Geosci. Model Dev.*, 4, 957-992, doi:10.5194/gmd-4-957-  
1310 2011, 2011.

1311

1312 Matthews, H.D. and Caldeira, K.: Transient climate-carbon simulations of planetary  
1313 geoengineering, *PNAS*, 104, 9949–9954, doi:10.1073/pnas.0700419104, 2007.

1314

1315 Mercure, J.-F., Pollitt, H., Chewprecha, U., Salas, P., Foley, A.M., Holden, P.B. and  
1316 Edwards, N.R.: The dynamics of technology diffusion and the impacts of climate  
1317 policy instruments in the decarbonisation of the global electricity sector, *Energy*  
1318 *Policy*, 73, 686-700, doi:10.1016/j.enpol.2014.06.029, 2014.

1319

1320 Micheels, A. and Montenari, M.: A snowball Earth versus a slush-ball Earth:  
1321 Results from Neoproterozoic climate modeling sensitivity experiments,  
1322 *Geosphere*, 4, 401-410, doi: 10.1130/GES00098.1, 2008.

1323

1324 Molteni, F.: Atmospheric simulations using a GCM with simplified physical  
1325 parameterizations. I: Model climatology and variability in multi-decadal  
1326 experiments, *Climate Dynamics*, 20, 175-191, 2003.

1327

1328 Oliver, K. I. C. and Edwards, N. R.: Location of potential energy sources and the  
1329 export of dense water from the Atlantic Ocean, *Geophys. Res. Lett.*, 35, L22604,  
1330 doi:10.1029/2008GL035537, 2008.

1331

1332 Oort, A.H.: Global atmospheric circulation statistics, 1958- 1973:NOAA Prof Pap  
1333 14, 1983.

1334

1335 [Pacanowski, R.: MOM 2 Documentation User's Guide and Reference Manual,](#)  
1336 [GFDL Ocean Group Technical Report. NOAA, GFDL, Princeton, 232pp, 1995.](#)

1337

1338 Plattner, G.-K., R. Knutti, F. Joos, T. F. Stocker, W. von Bloh, V. Brovkin, D.  
1339 Cameron, E. Driesschaert, S. Dutkiewicz, M. Eby, N. R. Edwards, T. Fichefet, J. C.  
1340 Hargreaves, C. D. Jones, M. F. Loutre, H. D. Matthews, A. Mouchet, S. A. Mueller, S.  
1341 Nawrath, A. Price, A. Sokolov, K. M. Strassmann, and A. J. Weaver 2008 Long-term  
1342 climate commitments projected with climate - carbon cycle models. *Journal of*  
1343 *Climate*, Vol. 21, pp. 2721-2751, doi: 10.1175/2007JCLI1905.1, 2008

1344

1345 Roscher, M., Stordal, F., and Svenson, H.: The effect of global warming and global  
1346 cooling on the distribution of the latest Permian climate zones, *Palaeogeogr.*  
1347 *Palaeocl.*, 309, 186–200, doi:10.1016/j.palaeo.2011.05.042, 2011.  
1348

1349 [Sarojini, B.B., Gregory, J.M., Tailleuc, R., Bigg, G.R., Blaker, A.T., Cameron, D.R.,](#)  
1350 [Edwards, N.R., Megann, A.P., Shaffrey, L.C. and Sinha, B.: High frequency](#)  
1351 [variability of the Atlantic meridional overturning circulation, \*Ocean Science\*, 7, 471-](#)  
1352 [486, doi:10.5194/os-7-471-2011, 2011.](#)  
1353

1354 Schmittner, A., Silva, T.A.M., Fraedrich, K., Kirk, E. and Lunkeit, F.: Effects of  
1355 mountains and ice sheets on global ocean circulation, *Journal of Climate*, 24, 2814-  
1356 2829, DOI: 10.1175/2010JCLI3982.1, 2010.  
1357

1358 Severijns, C.A. and Hazeleger, W.: The efficient global primitive equation climate  
1359 model SPEEDO V2.0, *Geosci. Model Dev.*, 3, 105-122, [www.geosci-model-](http://www.geosci-model-)  
1360 [dev.net/3/105.2010/](http://dev.net/3/105.2010/), 2010.  
1361

1362 [Slingo, A., and Slingo, J.M.: Response of the National Center for Atmospheric](#)  
1363 [Research community climate model to improvements in the representation of clouds.](#)  
1364 [J. Geoph. Res., 96, 341-357, 1991.  
1365](#)

1366 Talley, L.D.: Freshwater transport estimates and the global overturning circulation:  
1367 Shallow, deep and throughflow components, *Progress in Oceanography*, 78, 257-303,  
1368 doi:10.1016/j.pocean.2008.05.001, 2008.  
1369

1370 Trenberth, K.E., Smith, L., Qian, T., Dai, A. and Fasullo, J.: Estimates of the global  
1371 water budget and its annual cycle using observational and model data, *Journal of*  
1372 *Hydrometeorology – Special Section*, 8, 758-769, doi: 10.1175/JHM600.1, 2007.  
1373

1374 Trenberth, K.E., Fasullo, J.T. and Kiehl, J.: Earth's global energy budget, *Bulletin of*  
1375 *the American Meteorological society*, 90, 311-323, doi:10.1175/2008BAMS2634.1,  
1376 2009.  
1377

1378 Williams, J.H.T., Smith, R.S., Valdes, P.J., Booth, B.B.B. and Osprey, A.: Optimising  
1379 the FAMOUS climate model: inclusion of global carbon cycling, *Geosci. Model Dev.*,  
1380 6, 141-160, doi: 10.5194/gmd-6-141-2013, 2013.  
1381  
1382 Williamson, D., Blaker, A.T., Hampton, C. and Salter, J.: Identifying and removing  
1383 structural biases in climate models with history matching, *Climate Dynamics*, 45,  
1384 1299-1324, doi: 10.1007/s00382-014-2378-z, 2015.  
1385  
1386 Williamson, M.S., Lenton, T.M., Shepherd, J.G. and Edwards, N.R.: An efficient  
1387 numerical terrestrial scheme (ENTS) for Earth system modelling, *Ecological*  
1388 *modelling*, 198, 362-374, doi:10.1016/j.ecolmodel.2006.05.027, 2006.  
1389  
1390 Zickfeld, K., Eby, M., Weaver, A. J., Cressin, E., Fichefet, T., Goosse, H., Philippon-  
1391 Berthier, G., Edwards, N. R., Holden, P. B., Eliseev, A. V., Mokhov, I. I., Feulner, G.,  
1392 Kienert, H., Perrette, M., Schneider von Deimling, T., Forest, C. E., Joos, F., Spahni,  
1393 R., Steinacher, M., Kawamiya, M., Tachiiri, K., Kicklighter, D., Monier, E.,  
1394 Schlosser, A., Sokolov, A. P., Matsumoto, K., Tokos, K., Olsen, S. M., Pedersen, J.  
1395 O. P., Shaffer, G., Ridgwell, A., Zeng, N., and Zhao, F.: Long-term climate change  
1396 commitment and reversibility, *J. Climate*, 26, 5782-5809, doi: 10.1175/JCLI-D-12-  
1397 00584.1, 2013.  
1398  
1399

1400 **TABLES**

Parameter	Description	Range	Subjective tuning
APM (Sv)	Atlantic-Pacific moisture flux <del>adjustment</del>	0 to 0.32	0.2132
OVD ( $m^2s^{-1}$ )	Reference diapycnal diffusivity	$2 \times 10^{-5}$ to $2 \times 10^{-4}$	$1.583 \times 10^{-4}$
OHD ( $m^2s^{-1}$ )	Isopycnal diffusivity	500 to 5,000	1,937
SCF (dimensionless)	Wind stress scaling	2 to 4	3.788
ADRAG (days)	Inverse ocean drag	0.5 to 5.0	2.069
OP1 (dimensionless)	Power law for diapycnal diffusivity depth profile	0.5 to 1.5	0.8200

Phil Holden 8/4/16 15:07  
**Deleted:** correction  
 Phil Holden 8/4/16 15:07  
**Deleted:** m<sup>-2</sup>s  
 Phil Holden 8/4/16 15:07  
**Deleted:** m<sup>-2</sup>s

1401 **Table 1:** Ensemble varied parameters.

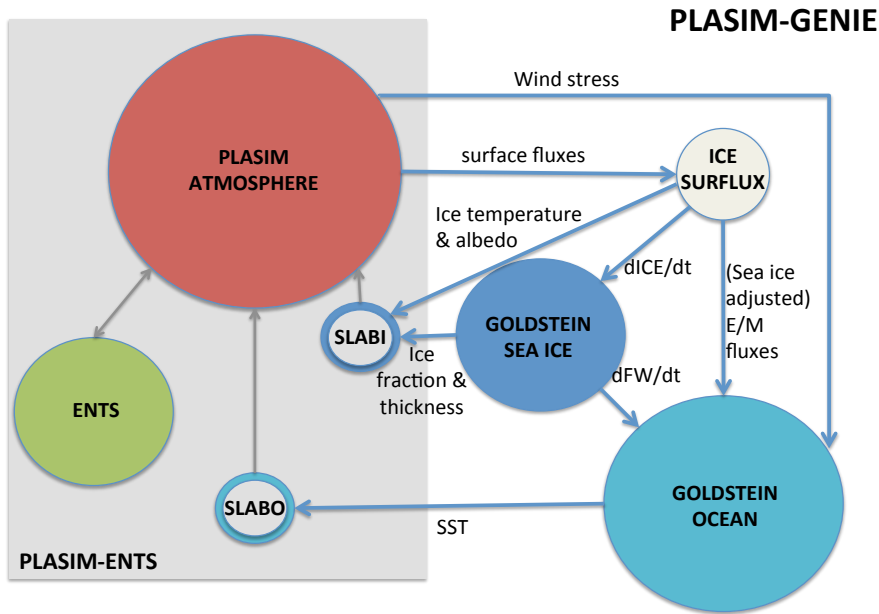
Solar radiation ( $Wm^{-2}$ )					
	Incoming TOA	Reflected by atmosphere	Absorbed by atmosphere	Reflected by surface	Absorbed by surface
PLASIM-GENIE	341	75	66	39	161
ERBE (1985-1989)	339-343	70-83	64-81	23-45	156-169
CERES (2000-2004)	339-342	69-82	64-78	23-45	161-170
Planetary radiation and heat fluxes ( $Wm^{-2}$ )					
	Sensible heat	Latent heat	Back radiation	Upward surface radiation	Outgoing radiation OLR
PLASIM-GENIE	20	78	323	386	228
ERBE (1985-1989)	15-24	78-85	324-345	390-396	235-254
CERES (2000-2004)	15-19	83-90	324-345	394-397	236-254

1402 **Table 2:** The global energy balance of subjectively-tuned PLASIM-GENIE in the  
 1403 preindustrial state compared against estimates derived from the 'Earth Radiation  
 1404 Budget Experiment' ERBE (1985-1989), when the Earth's radiation balance was in  
 1405 approximate equilibrium, and the 'Clouds and Earth's Radiant Energy System'  
 1406 CERES data (2000-2004). The observational uncertainties reflect a range of  
 1407 analyses summarised in Trenberth et al (2009).

Surface ocean moisture fluxes (Sv)						
	Atlantic/Arctic Ocean	Pacific Ocean	Indian Ocean	Southern Ocean	Total Ocean	Trenberth et al (2007)
Precipitation	1.96	4.76	1.67	2.89	<b>11.28</b>	11.8
Evaporation	-2.68	-5.48	-1.98	-2.52	<b>-12.66</b>	-13.1
Run off	0.59	0.36	0.23	0.18	<b>1.37</b>	1.3
Flux <del>adjustment</del>	-0.21	0.21	0.00	0.00	<b>0.00</b>	
<b>Net</b>	<b>-0.34</b>	<b>-0.14</b>	<b>-0.07</b>	<b>0.56</b>	<b>0.00</b>	
Talley (2008)	-0.28±0.04	0.04±0.09	-0.37±0.10	0.61±0.13		

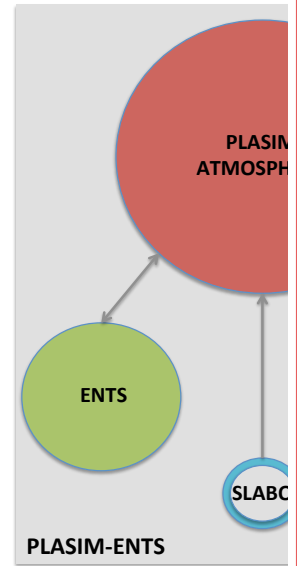
Phil Holden 8/4/16 15:07  
**Deleted:** correction

1408 **Table 3:** Simulated surface ocean moisture fluxes of the subjective tuning and  
 1409 observationally constrained estimates. The definition of ocean basin boundaries  
 1410 follows Talley (2008) viz. Atlantic and Indian Oceans north of 32°S, Pacific Ocean  
 1411 north of 28°S.

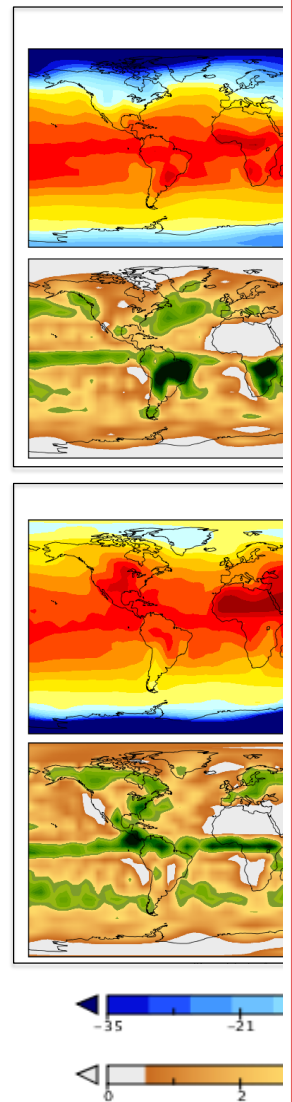


1417  
 1418  
 1419  
 1420  
 1421  
 1422  
 1423  
 1424  
 1425  
 1426  
 1427  
 1428

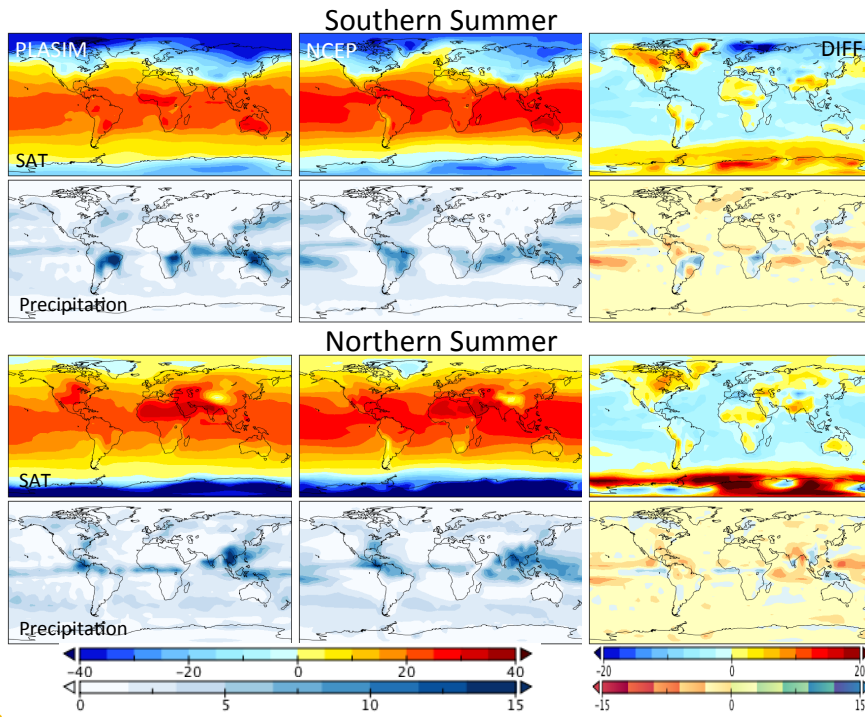
**Figure 1:** A schematic of the PLASIM-GENIE coupling. The circles represent the component modules, with sizes indicative of their relative complexity. The grey box defines the PLASIM-ENTS model, which has been retained in its entirety; hollow circles (SLABO and SLABI) are dummy PLASIM modules, retained only to specify ocean and sea-ice boundary conditions from GOLDSTEIN outputs; grey lines are energy and moisture fluxes that are calculated within the pre-existing PLASIM-ENTS coupling. Blue arrows are variables passed in the PLASIM-GENIE coupling. ICE-SURFLUX is the new surface flux routine that was developed for the coupling (see Section 3.3)



Deleted:  
 Phil Holden 8/4/16 15:07



Deleted:



1433  
1434  
1435  
1436  
1437  
1438

**Figure 2:** Seasonal surface air temperature (°C) and precipitation (mm/day). Left: PLASIM-GENIE 50-year average. Centre: long-term average (1981-2010) NCEP/NCAR reanalysis fields (Kalnay et al 1996). Right: difference (PLASIM-NCEP).

Unknown  
Formatted: Font:Bold

Phil Holden 8/4/16 15:07

Deleted: .

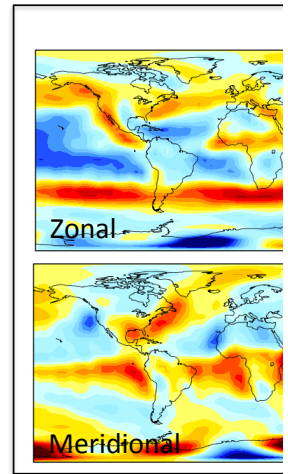
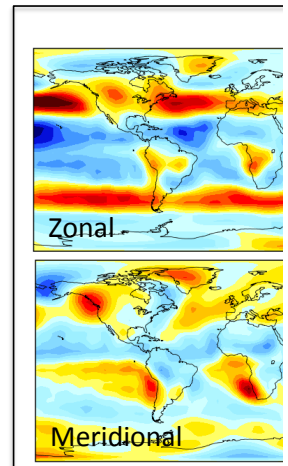
Phil Holden 8/4/16 15:07

Deleted: outputs (left) are compared with

Phil Holden 8/4/16 15:07

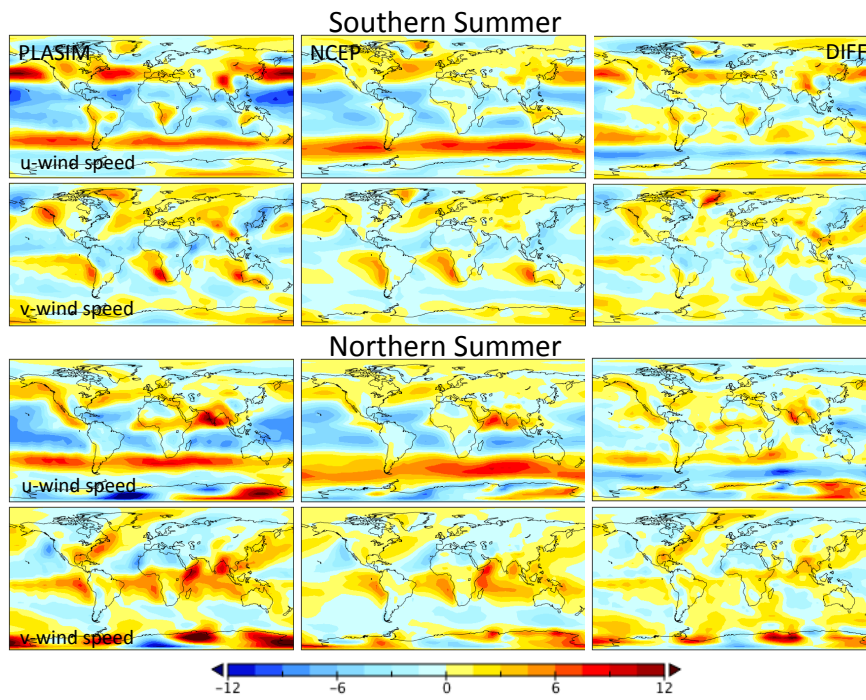
Deleted: right,

Phil Holden 8/4/16 15:07



Deleted: -10.0 ... [2]



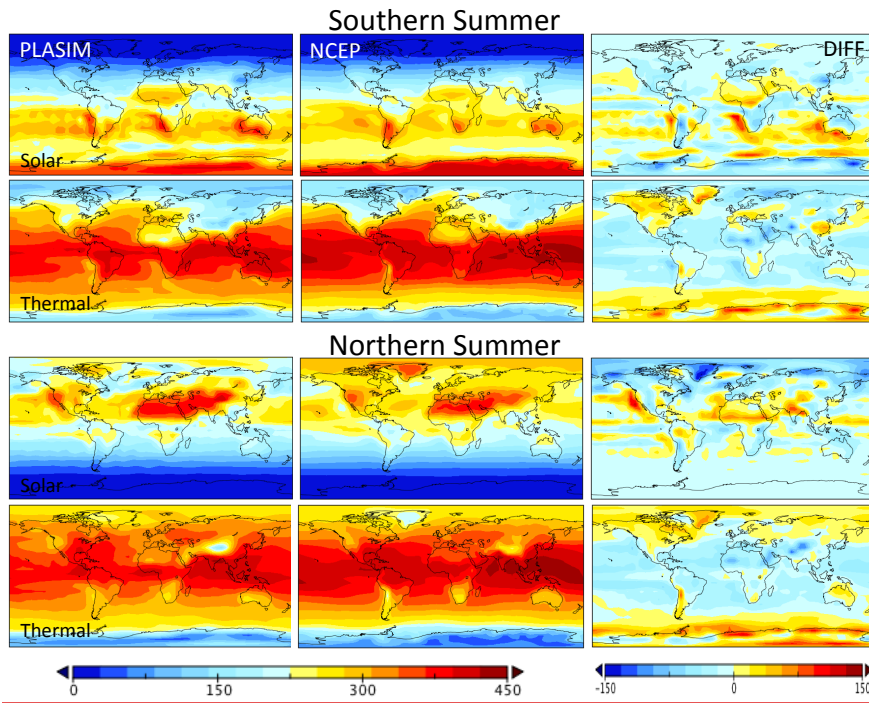


1444  
 1445  
 1446  
 1447  
 1448  
 1449  
 1450

**Figure 3:** Seasonal surface zonal and meridional wind speeds ( $\text{ms}^{-1}$ ). **Left:** PLASIM-GENIE 50-year average. **Centre:** long-term average (1981-2010) NCEP/NCAR reanalysis fields (Kalnay et al 1996). **Right:** difference (PLASIM-NCEP).

Phil Holden 8/4/16 15:07  
~~Deleted:~~ outputs (left) are compared with  
 Phil Holden 8/4/16 15:07  
~~Deleted:~~ right,

1453



1454

1455

1456

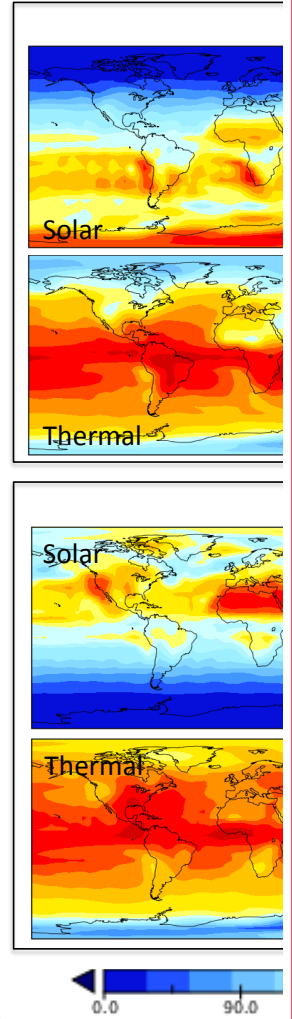
1457

1458

1459

**Figure 4:** Seasonal incoming surface solar and thermal radiation ( $Wm^{-2}$ ). Left: PLASIM-GENIE 50-year averages. Centre: long-term average (1981-2010) NCEP/NCAR reanalysis fields (Kalnay et al 1996). Right: difference (PLASIM-NCEP).

Phil Holden 8/4/16 15:07



**Deleted:**

Phil Holden 8/4/16 15:07

**Formatted:** Font:Bold

Phil Holden 8/4/16 15:07

**Deleted:** outputs (left) are compared with

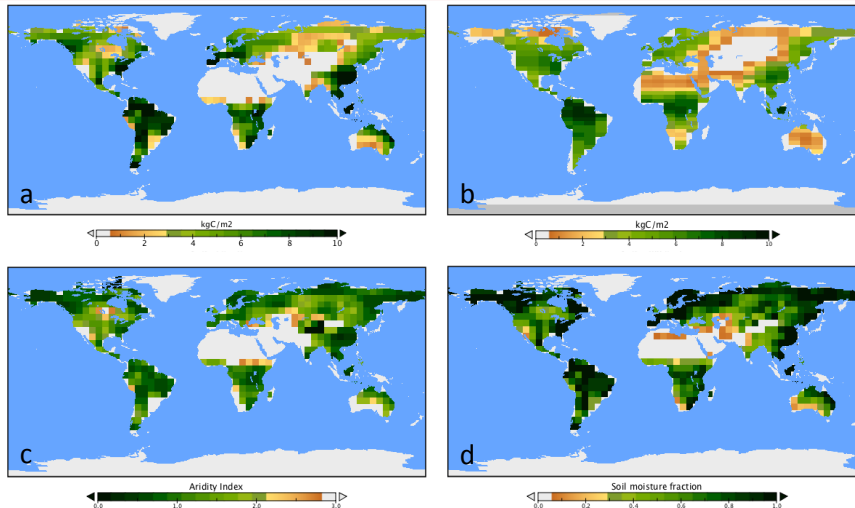
Phil Holden 8/4/16 15:07

**Deleted:** right,

Phil Holden 8/4/16 15:07

**Deleted:** Page Break

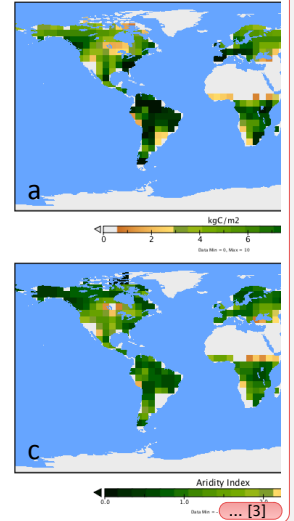
1464



1465  
1466  
1467  
1468  
1469

**Figure 5:** Land surface. a) ENTS vegetation carbon density from PLASIM-GENIE, b) ENTS vegetation carbon density from GENIE-1 (Holden et al 2013a), c) Budyko aridity index N/P and d) soil moisture fraction E/N

Phil Holden 8/4/16 15:07



Deleted:

Phil Holden 8/4/16 15:07

Deleted: soil

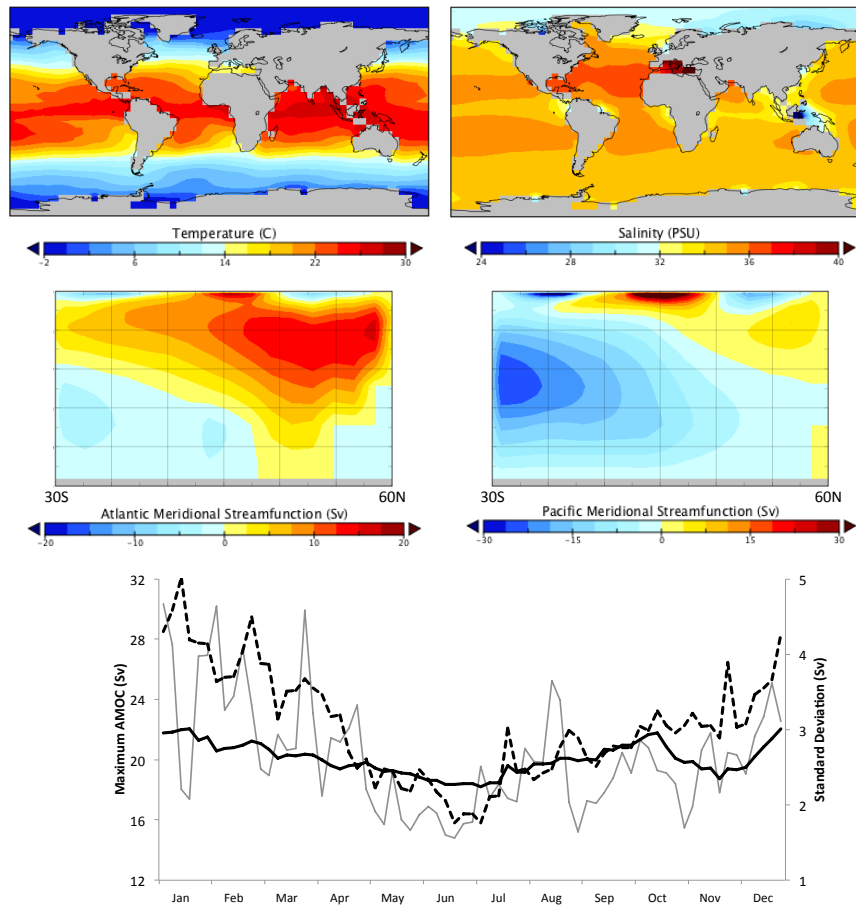
Phil Holden 8/4/16 15:07

Deleted: ,

Phil Holden 8/4/16 15:07

Deleted: .

1475  
1476  
1477



1478  
1479  
1480  
1481  
1482  
1483

**Figure 6:** Ocean. Upper panels: PLASIM-GENIE simulated surface ocean temperature and salinity. Central panels: PLASIM-GENIE simulated Atlantic and Pacific meridional stream functions. Lower panels. Wind-driven AMOC variability: solid black 100-year mean, dashed black 100-year standard deviation, solid grey arbitrary year (year 100 of a spin-on simulation)

Phil Holden 8/4/16 15:07

**Deleted:** Lower